Title
An Optimization Framework for Two-tier Cellular Network Resource Allocation and Handover

Author
Li, Wuwen

Publication Date
2019

Peer reviewed|Thesis/dissertation

UNIVERSITY OF CALIFORNIA

Los Angeles

An Optimization Framework for Two-tier Cellular Network Resource Allocation and Handover

A dissertation submitted in partial satisfaction
of the requirements for the degree
Doctor of Philosophy in Electrical and Computer Engineering

by

Wuwen Li

2019

ABSTRACT OF THE DISSERTATION

An Optimization Framework
for Two-tier Cellular Network Resource
Allocation and Handover

by

Wuwen Li
Doctor of Philosophy in Electrical and Computer Engineering
University of California, Los Angeles, 2019
Professor Gregory J. Pottie, Chair

The Orthogonal Frequency Division Multiplexing Access (OFDMA) and macro-femto two-tier heterogrneous network are the core technologies used in 4G and 5G cellular networks. These pose new challanges and optimization potential for network resource allocation with consideration of fairness as well as for user equiptment (UE) handoff with consideration of resource allocation. This thesis studies both problems, and analyses the inherent difficulties in the problem domain. Then several optimization algorithms are proposed to solve the problem. An optimization framework is proposed to integrate the algorithms together.

The dissertation of Wuwen Li is approved.

John D. Villasenor

Danijela Cabric

Babak Daneshrad

Gregory J. Pottie, Committee Chair

University of California, Los Angeles

2019

To my wife ...

Rachel Wu for all her support

TABLE OF CONTENTS

LIST OF FIGURES

LIST OF TABLES

ACKNOWLEDGMENTS

I would like to show my deepest gratitude to my supervisor, Greg Pottie, a respectable, responsible and resourceful scholar, who has provided me with valuable guidance in every stage of the writing of this thesis. Without his enlightening instruction, impressive kindness and patience, I could not have completed my thesis. His keen and vigorous academic observation enlightens me not only in this thesis but also in my future career.

I shall extend my thanks to my mother Yindi Jiang for all her kindness and support. I would also like to thank my father, Zhongyi Li even though he could not see me reaching to this point. He was the first person who encouraged me to go down this path, guided me to develop the fundamental and essential academic competence.

Last but not least, I' d like to thank my wife Rachel Wu, for her loving considerations and great confidence in me all through these years.

VITA

1997	B.S. (Computer Science), The Center University Of Nationalities.
1997–1998	Software Engineer, Founder Information System Corporation, China.
1998–1999	Software Engineer, Hitachi Semiconductor America, China Design Center.
1999–2001	DSP Firmware Engineer, Nokia Mobile Phones, Finland.
2001–2006	DSP Firmware Engineer, Nokia Mobile Phones, San Diego, USA.
2006–2010	Senior Staff Engineer, Broadcom Bluetooth System Design, USA.
2011	M.S. (Engineering), UCLA, Los Angeles, California.
2012–2014	Principal Engineer, VTI Instrument Inc. USA.
2014–2016	RFSW Engineer, Qualcomm Inc. USA.
2016–present	Founder and CTO, Tanteq Co. ShenZhen, China.

PUBLICATIONS

2014 Information Theory and Applications Workshop (ITA), San Diego, CA, 2014, pp. 1-7. Fair resource allocation for OFDMA multi-cell networks

2019 Information Theory and Applications Workshop (ITA), San Diego, CA, 2019. A Machine Learning Based Optimization Framework for Macro-Femto Cellular Network Handover

Submitted to IEEE Transactions on Vehicular Technology, March, 2019. Distributed Multi-Cell Network Channel Allocation with Max-Min Fairness and Interference Avoidance

CHAPTER 1

Introduction

The fourth-generation (4G) of wireless cellular networks based on orthogonal frequency-division multiplexing (OFDM) technology has been deployed globally in the time since its first deployment in 2009. The proliferation of mobile wireless communication applications has drastically increased the market capacity for mobile devices and produced high demand for network bandwidth and link quality. Encouraged by the commercial success of the 4G wireless service, 5G networks are designed to meet these requirements.

It is highly likely that 5G will operate at higher frequencies, such as 28 GHz or 39 GHz. Small cells, including femto cells, will be critical at these millimeter wave frequencies. This is because the signals cannot penetrate walls or buildings and the cell sizes will have a coverage radius of less than 500 meters. Therefore the 5G network will consist of small cells rather than macro cells and it will not be a replacement to 4G but work in parallel. It is reasonable to conjecture that the mobile communication network is evolving towards a macro-femto two-tier heterogeneous network.

The diversity in the applications and the two-tier heterogeneous network structure pose strong challenges for network resource allocation with quality-of-service (QoS) awareness, as well as requiring a better handover algorithm.

1.1 Cases Considered

This section describes the specific cases that were studied. These include: uniform multi-cell macro networks uplink resource allocation, random sized multi-cell macro networks uplink resource allocation and macro-femto two-tier networks UE handover with resource allocation

considered. Within the first two cases, UE does not perform handover when it moves out of the cell boundary.

1.2 Contribution

The objective of this thesis is to analyze the inherent problem in resource allocation in the multi-cell macro network and propose a fully distributed resource allocation algorithm with max-min fairness and interference avoidance. With the algorithm in place, a higher level optimization framework is constructed that considers handover performance optimization and resource allocation all together. Both optimization algorithms should be adaptive to environmental dynamics and distributed with minimum information exchanged among cells.

First the thesis proposes a novel spectrum efficiency and fairness multi-criterion optimization model for multi-cell OFDMA networks uplink channel allocation. The model is then transformed into an integer programming problem and a branch-cut based algorithm is proposed to solve it. To tackle the inherent coupling problem between inter-cell-interference (ICI) estimation and resource allocation in the optimization, a distributed dynamic uplink channel allocation algorithm is proposed. The algorithm requires no runtime inter-cell information exchange. In the algorithm, the base station (BS) initially has the maximum uncertainty (entropy) over the channel ICI. The BS reduces the entropy by viewing ICI measurement as an information source. The more information extracted, the more channel ICI distribution knowledge is gained. The ICI distribution is used to calculate the channel average interference and then the channel preference value (CPV) is derived. Higher CPV makes the corresponding channel more likely to be used. When neighbor cells' traffic change, environmental ICI may change. Using the algorithm, the BS learns the environmental dynamics and updates its CPV opportunistically. A two-dimensional simulation conducted on both uniform and random-sized-cells shows the benefits are significant.

Secondly, we tackle the challenges posed by the macro-femto two-tier heterogeneous cellular network on user equipment (UE) handover (HO) management. The thesis proposes to consider multiple parameters that affect the HO process in a uniform framework and to

be able to dynamically adapt to the environment. The thesis proposes a machine learning based optimization framework for HO control. The framework has a three-tier structure including data sample selector (DSS), learning agent (LA), and handover controller (HOC). The three components form a closed-loop control system that collects data samples from the HO process. Data samples are scrutinized and then stored in the training data set (TDS), which is used to train the LA. The LA first determines data sample distance weight factors by studying the TDS and then employs a weighted KNN algorithm to dynamically adjust HO control parameters. Simulation results show that our proposed framework is more effective in both macro to femto and femto to femto scenarios compared to conventional HO algorithms.

1.3 Organization

The remainder of this thesis is organized as follows. Chapter 2 presents some technical background that is used in the development of the algorithms in this thesis. Chapter 3 explains the resource allocation problem and our solution, including problem formulation, algorithm explanation and simulation results discussion. Chapter 4 explains the machine learning based handover optimization framework, including optimization formulation, algorithm explanation and simulation results discussion. Chapter 5 presents our conclusions and suggestions for future work.

CHAPTER 2

Technical Background

In this chapter we provide an overview of a number of algorithms used for key computations in later chapters of the thesis.

2.1 Linear Programming and Integer Programming

2.1.1 Introduction to Linear Programming

Linear programming (LP) minimizes or maximizes a linear objective function subject to a set of linear constraints. A linear objective function is a linear equation formed by a group of variables. The goal is to identify the variable values that minimize or maximize the objective function while also satisfying the specified linear constraint equations. An LP example is given below:

$$\text{Maximize: } c_1X_1 + c_2X_2 + c_3X_3 \tag{2.1}$$

$$\text{Subject to: } a_1X_1 + a_2X_2 + a_3X_3 \leq b \tag{2.2}$$

X_1, X_2, X_3 are variables. $c_1, c_2, c_3, a_1, a_2, a_3, b$ are constants. The objective of this example is to identify the X that maximizes equation (2.1) while also satisfying equation (2.2).The set of variable values that satisfy the constraints is called the feasible set or feasible region. Integer programming (IP) differs from linear programming only in the additional requirement that every variable has an integer value.

2.1.2 Solving Integer Programming

Every IP problem has an associated LP problem, called its linear relaxation, formed by eliminating the integrality restrictions. In the other words, the LP relaxation has the same objective and constraint equations as the original IP problem. However, the variables in the LP relaxation are allowed to take non-integer values. Let S(IP) and S(LP) denote the solution to the IP problem and its linear relaxation respectively. They have following relationship:

(a) S(IP) cannot be a more desirable value of the objective function than S(LP).

(b) IP must be infeasible (i.e. have an empty feasible set) if its linear relaxation is infeasible.

(c) Given that the objective function coefficients are integers, we have $S(IP) \geq \lceil S(LP) \rceil$ for minimization and $S(IP) \leq \lfloor S(LP) \rfloor$ for maximization.

The IP problem is called *infeasible* if the feasible set is empty. IP usually is solved by two algorithms described in following sections.

Branch and Bound Algorithm This algorithm is described as:

(a) Solving IP relaxation LP to get S(LP). If S(LP) are all integers, then S(LP) = S(IP). Otherwise, we need to split the original IP problem into two subproblems by taking one of the variables in the LP solution that has a non-integer value and adding one of two constraints that each make that non-integer value impossible while still preserving all integer solutions. This is called branching.

(b) A subproblem is not active if the conditions of it have been used to branch on, its S(LP) = S(IP), the subproblem is infeasible, or its S(LP) is less optimal than a currently obtained integer solution.

(c) Selecting an active subproblem to branch on a fractional variable.

The branching method used in the algorithm is to select one of the variables with a fractional value and then add two additional constraints to bound the variable to the floor and

ceiling of the solution. For example, for x=3.37, applying the branching algorithm, we would branch it into two subproblems (nodes) and add constraints $x \leq 3$ and $x \geq 4$ respectively.

The idea is to repeat the above three steps until there are no active subproblems. During the whole process, the current best solution is tracked. Subproblem nodes, whose optimal solution is less optimal than the current most optimal solution, are dropped (declared inactive). This procedure is called bound. A subproblem is *fathomed* if the LP at the node is infeasible, S(LP) = S(IP) at the node, or S(LP) is bounded away from the current best solution. The algorithm reports the current optimal solution as the best solution once all the nodes are covered.

Cutting Plane Algorithm The cutting plane algorithm is an alternative IP-solving method to the branch algorithm. The idea behind this method is to add constraints, which are called cuts, to the LP until the optimal solution takes on integer values. Care must be taken not to change the original IP by adding these cuts to the LP. The sole purpose of adding cuts is to eliminate fractional solutions so that LP solution finally converges to the optimal integer solution.

Therefore a valid cut must satisfy following two conditions:

(a) The new IP feasible region must be equal to the original IP feasible region.

(b) A current fractional solution must be eliminated by the cut.

The procedure to generate the cut more or less depends on the specific application. Figure 2.1 illustrates the cutting-plane concept. The black dots represent all the feasible IP integer solutions. The red dot represents a fractional solution. A valid cut is added on the plane to exclude just the fractional solution (red dot), while keeping all the black dots in the feasible region.

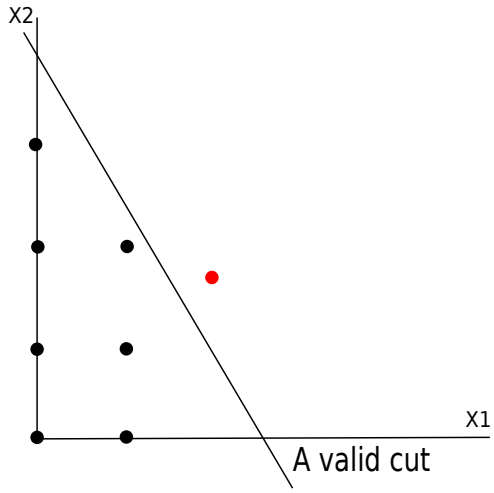

Figure 2.1: A valid cut to eliminate fractional solution

2.2 Relative Entropy

Relative entropy (also called Kullback-Leibler divergence) is used in the thesis to measure how different one probability distribution is from another [Ash90]. Since this thesis exploits discrete probability to model the channel interference level, we explain the concept of relative entropy using discrete probability distributions. Assuming P and Q are two discrete probability distributions on the same probability space, the relative entropy from Q to P is defined to be:

$$D(P//Q) = \sum_i P(i)\ log\left(\frac{P(i)}{Q(i)}\right) \tag{2.3}$$

The $D(P//Q)$ is the expectation of the logarithmic difference between P and Q, where the expectation is taken using probability P. Therefore the relative entropy cannot be regarded as a true distance between P and Q since it is not symmetric. However, it fits our need in this thesis well. The algorithm keeps a belief on channel interference level and relies on relative entropy to decide when to adjust the belief. In the other words, the relative entropy is a measure of surprise. The algorithm should change its belief if the surprise is above a threshold.

2.3 Machine Learning: K-Nearest Neighbors Algorithm

The K-Nearest Neighbors (KNN) algorithm classifies data points based on the distance measured between data features. KNN is one of the simplest machine learning algorithms. The principle used by KNN to classify data points is to find the closest data group in terms of data feature distance. When KNN does its job, it consults the K nearest neighbors for their opinions. The classification decision goes with the majority neighbors' classification. Figure 2.2 shows an example with K=7.

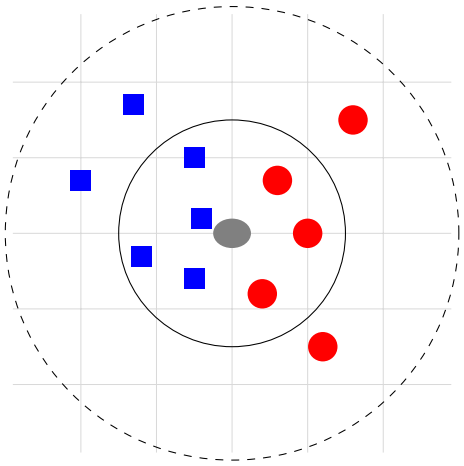

Figure 2.2: K=7 nearest neighbor classifier

In the above example, the ellipse represent a new data point to be classified. KNN checks 7 nearest neighbors and sees that there are 4 data points belonging to the square class and 3 data points belonging to the round class. Therefore the new data point should be classified into the square data group. A KNN algorithm has steps as follows:

- compute the distance between the given new data point and other existing points
- find the K nearest neighbors from all existing points
- assign the new data a class

The KNN algorithm is easy to understand and implement. There is no need for algorithm training. The data point distance computation is one of the key components in the KNN

algorithm performance. In the later section of this thesis, we will explain how to compute the data point distance in the case studied. The other critical performance related parameter is the vote evaluation. We have improved on that aspect by adding a weight factor for each vote. The weight factor is derived from the degree that the class members are consistent in their agreement. See [SH10, YY06, YI03] for detailed explaination about KNN.

CHAPTER 3

Distributed Network Channel Allocation

3.1 Introduction

In recent years, OFDMA networks have been increasingly deployed in various cellular networks. With increasing network density and user traffic load, efficient fairness-constrained resource allocation becomes critical. In this chapter, we focus on distributed dynamic uplink channel allocation in OFDMA multi-cell networks. It is known that allocating channels to users with the maximum marginal rate maximizes the network throughput [LL05],[MTB10],[KHK05]. However, since some users may be in deep fading, there are advantaged and disadvantaged users. Simply maximizing the network throughput will always starve disadvantaged users. Therefore, fairness constrained throughput optimization is desired. Max-minimum fairness as proposed in [HL14] is used in our study.

Resource allocation algorithms face two major difficulties. First, many existing multi-cell resource allocation algorithms require inter-cell information exchange [YDH13], [MTB11], [NDN16]. A distributed algorithm with minimum inter-cell information exchange is always desired. Second, in a multi-cell network, the environment of a cell is not always steady due to the user traffic dynamics in neighbor cells. Dynamic adaptive resource allocation is often needed to address this issue. However, dynamically reallocating resources in different cells without centralized coordination makes the inter-cell-interference-power-spectrum (ICIPS) unpredictable. In other words, it is an inherent coupling issue that measurement based decisions cause measurements to change. This measurement-decision-coupling (MDC) issue is one of the most significant challenges that any practical distributed algorithm needs to face. This is very similar to the problem studied by second order chaotic system (SOCS)

in the dynamical systems theory. The SOCS is extremely unpredictable because the system does respond to the prediction, e.g. the stock market. Even though we do not prove that the system studied in this chapter is chaotic, we do attempt to analyze the problem from the dynamical systems point of view.

The novelties of our work are: i) A new resource allocation optimization formulation to improve spectrum efficiency and max-minimum sense of user fairness. The optimal solution is found by first transforming the model into a zero-one integer programming (ZOIP) formulation which is then solved by the branch-cut algorithm. It is a truly distributed dynamic channel re-allocation approach that requires no inter-cell information. ii) To tackle the MDC problem, a channel preference vector (CPV) derived from ICIPS is used by each cell to determine the channel preference for assignment. A dynamic CPV updating algorithm (DCUA) is invented to perform ICIPS tracking and CPV determination tasks. It does it in microscopic and maroscopic levels with the help of models from a dynamical systems view point. At the microscopic level, the algorithm estimates the ICI level for a single channel. It initially assumes a uniform probability distribution over all possible interference levels for every single channel. At this point, the cell has the maximum uncertainty (entropy) on channel interference level. Each cell starts to measure the ICIPS periodically and considers it as an information source. For each channel, the cell periodically checks relative entropy between its interference-level-distribution (ILD) assumption and the measured ones and uses that to determine whether its belief matches the reality. The cell also sees ICI as an information source and tracks its mutual information to determine environment steadiness. Based on this information, the algorithm gradually adjusts its channel ILD and then computes the average interference level for each channel. At the macroscopic level, the algorithm takes a holistic approach and models the ICIPS vector variation process as a phase point trajectory in a dynamical system phase space. It exploits the ICIPS uncertainty to skip transient ICIPS fluctuations and stabilizes CPV derivation. The goal is to let neighbor cells have their CPV isolated from each other and make the CPV adjustment in a stable environment. Hence, the cell avoids running optimization based on instantaneous ICIPS measurements and reallocating channels simultaneously with its neighbors.

In the rest of the chapter, we first revisit existing research work. Then we describe the two network models we used and formulate the optimization problem. We then present the details of the branch-cut algorithm to solve the optimization. Next the DCUA algorithm is explained. Finally, our simulation results are presented.

3.2 Related Work

The majority of prior research on the channel allocation algorithm considering ICI reduction can be grouped by the following criteria: static or dynamic algorithm, centralized or distributed, iterative or non-iterative.

Fixed channel allocation (FCA), fractional frequency reuse (FFR) and soft frequency reuse (SFR) are static bandwidth allocation algorithms. They reduce ICI by pre-planning the channels among adjacent cells [KN00], [YD12], [HKH13] and [YDH12a]. Fixed channel allocation algorithms have low spectral efficiency, since they do not dynamically adapt to network traffic load variation. Dynamic channel allocation (DCA) techniques were invented to address this issue. Channel segregation (CS) is such an algorithm explained in [KN00]. CS prioritizes all channels and employs a learning algorithm to update the channel priorities according to the channel historical utility information. However, the learning algorithm does not consider transient ICI variation. In addition, in a multi-cell network, adjacent cells adjusting channel allocation simultaneously makes ICI even more unpredictable. We found the impact of this problem in our preliminary work [LP14a], but did not address it with a proper solution. A successful solution is presented here. [CWZ12] introduced a soft frequency reuse scheme for dense femtocell networks. The proposed algorithm first identifies multiple dominant interferers from the network and then classifies them into groups. Next, different frequency reuse factors and transmit powers for these groups are adjusted adaptively to mitigate the mutual interference. Among many dynamic frequency reuse schemes and interference mitigation approaches, graph-based methods are an important branch. [VK15] models the network in a graph and then introduces local games on it to optimize the network capacity. A semi-centralized dynamic frequency reuse scheme is introduced in [PSQ12], which

incorporates graph-coloring and network utility concepts on top of intra-cell scheduling to mitigate ICI. [ZHJ13] proposed a User-oriented Graph based Frequency Allocation (UGFA) algorithm. UGFA improves frequency reuse rate by exploiting graph based partitions on an interference graph for the users in the network. Comparing to classical adjusting frequency reuse factor methods aforementioned, our approach is more autonomous and completely decentralized. Thus our approach is more flexibly and able to adapt to the environmental changes.

For multi-cell networks, resource allocation is performed by centralized authorities. One way to do it is to organize cells into clusters and have the radio network controller (RNC) allocate channels to users in different cells. RNC will make sure two adjacent cells do not allocate the same channel to their users [LCB12]. A similar approach is taken by [YDH12b]. The difference is that [YDH12b] only assigns disjoint channels to cell edge users. Users in the cell center area can be assigned any channels. The requirement of using a centralized network controller limits its application to networks like femto cells and sensor networks. Therefore distributed channel allocation algorithms are favored in general. There are two major approaches: game-theory-based and graph-based [PSQ13]. Game-theory-based algorithms usually define utility functions, action sets and players corresponding to user data rate, resource allocation and network node or users respectively [LCS12], [WXS06] and [LCK08]. The solution is usually obtained by an iterative algorithm, which is in general inefficient. A graph-based channel and power joint allocation algorithm is described in [YDH13]. Users are represented by nodes in the graph. Two users are connected by an edge if they may interfere each other. Then the graph is colored and channels are allocated according to colors to avoid interference. In [WCT17], a bipartite graph is constructed between BSs and UEs. Then the Hungarian algorithm is employed to maximize network sum rate. In [KKL15], an impractical but theoretically optimal algorithm is proposed to solve the multi-cell resource allocation problem. Other than the aforementioned works, [LPM09, LRP17, KRS16] implement proportional fairness by applying a weight, which is inversely proportional to each UE's average data rate, in the resource allocation algorithm. [MNM16] proposes a resource allocation algorithm depending on measured channel gain. It also assumes each BS has full

information about channel gain. [KNH17] recognizes ICI as a major issue in OFDMA networks and proposes a resource allocation algorithm to mitigate ICI. The algorithm relies on decoding channel state information (CSI) broadcast to do channel prediction. Due to the signal propagation loss, only partial CSIs can be collected, which inevitably jeopardizes the performance of the algorithm. [MAP16] proposes sending network coordination information via back-haul links. The coordination information includes channel distribution information used by the resource allocation algorithm. [GFR18] proposes a round-robin (RR) algorithm to allocate channel resources in a fair time-sharing approach. [SYN17] proposes a ICI mitigation algorithm that requires each BS to exchange CSI in back-haul links.

To the best of our knowledge, there is no study that has suggested any truly distributed channel allocation algorithms for multi-cell OFDMA network that also resolves the MDC problem. Rather, the MDC problem is usually neglected in construction of distributed algorithms.

3.3 System Model

We describe the system model in three aspects: network model, channel propagation model and user data traffic and mobility model.

The network model used is a multi-cell, uniform-sized-cells (USC) OFDMA network. Each cell has three sectors and a fixed number of channels. As shown in Figure 3.1, there are 3 sectors colored in red for cell 1 at the center. The sector base station (BS) antennas point to 60, 180 and 270 degrees counter clockwise from horizontal line crossing the BS tower. This model is suggested in [RSS10a, Sec. 20.9] for LTE network simulation.

Within each sector, channels are assigned to user equipments (UE) for transmission. We only study the uplink, UE to BS. The other network layout studied for comparison is the random-sized-cells (RSC) network as shown in Figure 3.2. For RSC, BS' are randomly located according to a Poisson-Point-Process (PPP) following the model used in [SAV12], [GH09] and [GBA12]. Figure 3.2 shows RSC BS locations.

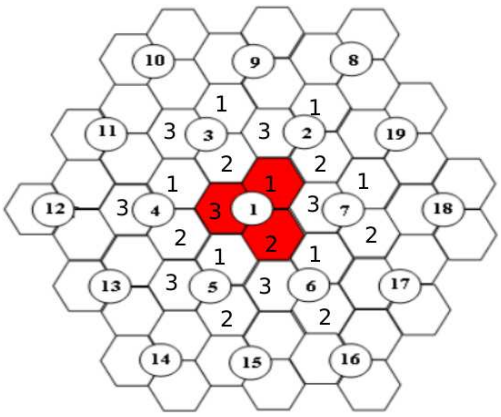

Figure 3.1: USC Network Layout

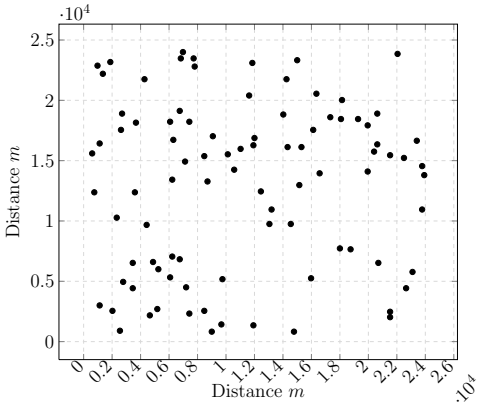

Figure 3.2: RSC Network Layout

We use the geometry based stochastic WINNER II channel model (W2CM) [P 08]. The channel model is a stochastic model with two levels of randomness. It includes Large-Scale Parameters (LSP) like shadow fading (SF), delay and angular spreads and Small-Scale Parameters (SSP) like delays, powers and directions of arrival and departure. All these parameters are drawn randomly from tabulated distribution functions. There are two types of parameter correlations modeled in W2CM LSP. At first, different parameters have cross-correlations C_{xy}. W2CM includes a LSP correlation table for different communication scenarios, i.e. indoor or outdoor. Next, for multi-link simulation, which is the case in this thesis, LSPs are correlated between neighbor links of UEs located close to each other. W2CM uses exponential correlation functions $\rho(d) \propto e^{-\frac{d}{\delta}}$, where $\rho(d)$ is the correlation coefficient, d is the distance between two UEs, δ is the correlation distance, to describe dependence of LSP

changes over distance. LSP also supports line-of-sight (LOS) to non-LOS (NLOS) transition control. The probability of existence of a LOS link is calculated from one of the W2CM tables for selected scenarios. The transition between LOS and NLOS leads to different path loss models. As to antenna gain, signal arrival angles (AoA) and departure angles (AoD) are generated. W2CM provides the probability function to generate these two parameters. Both AoA and AoD are used in the azimuth antenna pattern for gain computation. Additive white Gaussian noise (AWGN) is added to model thermal noise and radio links from neighbor cells are modeled as inter-cell interference (ICI). In the other words, neighbor cell UEs are regarded as interferers on the channels used by them for the home cell UEs. W2CM is used to calculate the ICI signal power from interferers using their distances to the home BS antenna. Finally ICI and AWGN are used in signal-to-noise ratio computation.

Poisson arrival models are used in this chapter for the user traffic model. When simulation starts the number of UEs for each cell is generated with a uniform distribution with its mean being a configurable simulation parameter. It remains constant during a simulation run. All UEs in the network have mobility with a random direction model described in [Bet01].

3.4 Problem Formulation

The optimization goal is to maximize the average spectral efficiency of a sector (E_s) (bits/s/Hz) and the minimum UE traffic rate R_{min}.

To formulate the E_s, we define $U = \{u_1, u_2, \dots\}$ as the set of all UEs in the network. Let $S = \{s_1, s_2, \dots\}$ be the set of all sectors in the network, and $s(u) = 1$ if the sector s is the home sector of $u(u \in s)$, otherwise $s(u) = 0$. In each sector, we assume there are in total N channels denoted by $C = \{c_1, c_2, \dots\ c_N\}$. Then using the Shannon capacity formula for the Gaussian channel, assuming bandwidth to be 1 for simplicity, the data rate of UE u on channel c is: $R_{s,cu} = v_{s,c}s(u)log_2(1 + \frac{G_{s,u}P_t}{I_{s,c}})$, $G_{s,u}$ is the propagation gain, P_t is the UE nominal transmission power, $I_{s,c}$ is the interference from neighbor sectors measured by sector s on channel c. $v_{s,c} \in [0, 1]$ is the channel CPV that enables algorithm 4 to give impact to algorithm 3. Both algorithms will be explained in the later sections.

We next define the sector s' channel allocation matrix A_s. Let $U^s = \{u_i | u_i \in s, (1 \leq i \leq |U|)\}$ be the UE set of sector s. A_s is a $N \times |U^s|, \{0, 1\}$ valued channel allocation matrix, with $A_s(c, u) = 1$ denoting that channel c is assigned to u ($u \in U^s$). Then we have $I_{s,c} = \sum_{s'} \sum_u s'(u) A_{s'}(c, u) G_{s,u} P_t, (s \neq s')$. Now we can define UE traffic rate matrix R_s, which is $N \times |U^s|$ real matrix, its element $R_s(c, u)$ is the achievable traffic rate of UE u on channel c. Therefore sector s' total sum of rate is $\sum_c \sum_u a_{s,cu} r_{s,cu}$, $(a_{s,cu} = A_s(c, u), r_{s,cu} = R_s(c, u))$. The total number of channels used is $\sum_c \sum_u a_{s,cu}$.

The spectral efficiency of sector s is defined by $E_s(A_s) = \frac{\sum_c \sum_u a_{s,cu} r_{s,cu}}{\sum_c \sum_u a_{s,cu}}$. The optimization model is defined as follows:

$$\max_{A_s} \quad E_s + \alpha R_{min} \tag{3.1}$$

$$\textbf{s.t.} \quad A_s \vec{\mathbb{1}} \preceq \vec{\mathbb{1}} \tag{3.2}$$

$$\vec{\mathbb{1}}^T A_s \succeq \vec{\mathbb{1}}^T \tag{3.3}$$

$$R_{min} = \min(diag(A_s^T R_s)) \tag{3.4}$$

$$\vec{\mathbb{1}}^T A_s P_t \preceq \vec{\mathbb{1}}^T P_{max} \tag{3.5}$$

$$A_s \text{ is 0 or 1 valued matrix} \tag{3.6}$$

where R_{min} is the minimum user traffic rate calculated by providing UE rate vector to function $min()$, which simply returns the smallest rate element from the rate vector. Eq. (3.2) makes sure one channel is assigned to at most one UE. Eq. (3.3) makes sure one UE gets at least one channel assigned. Eq. (3.5) assures UE transmission power does not exceed up limit P_{max}. We do believe that by constructing R_s using different transmission power P_t, power control optimization can be incorporated into the optimization model. It would be an interesting dimension of optimization on top of the current ones for future research.

The parameter $\alpha \geq 0$ is the weight factor to balance the gain in E_s and fairness. This is a multi-criterion optimization model.

3.4.1 Formulation Simplification and Solving Algorithm

Formulation (3.1) is a ZOIP since the optimization variable A_s is a {0,1} valued matrix. It is nonlinear because Eq. (3.4) and E_s are nonlinear. It is hard to solve a formulation like this analytically in general. We attempt to solve it by first constructing a similar but simplified model namely M^i. Its objective is to solely maximize E_s^i with a new constraint on the minimum rate. Then we solve a sequence of $M = \{M^0, M^1, \ldots, M^n\}$, where M^0 is given an initial value for R_{min}^0. Solving every following M^i yields R_{min}^i, which is always greater than R_{min}^{i-1}. M^i needs to be a linear model to take advantage of sophisticated linear programming (LP) algorithms. We first implement an initial channel allocation algorithm 1 to obtain an initial minimum rate value R_{min}^0. Once R_{min}^0 is obtained, next the nonlinear constraint (3.4) needs to be dropped. We reformulate (3.1) as:

$$\max_{A_s} \quad E_s^i \tag{3.7}$$

$$\textbf{s.t.} \quad A_s \vec{\mathbb{1}} \preceq \vec{\mathbb{1}} \tag{3.8}$$

$$\vec{\mathbb{1}}^T A_s \succeq \vec{\mathbb{1}}^T \tag{3.9}$$

$$diag(A_s^T R_s) \succ \vec{\mathbb{1}} R_{min}^{i-1} \tag{3.10}$$

$$\vec{\mathbb{1}}^T A_s P_t \preceq \vec{\mathbb{1}}^T P_{max} \tag{3.11}$$

$$A_s \text{ is 0 or 1 valued matrix} \tag{3.12}$$

Algorithm 1 Initial Channel Allocation

1: Let U = number of UEs in the cell
2: Pick U top channels according to CPV
3: Sort users according to their $G_{s,u}$ to BS
4: Perform a water filling channel allocation to assign one channel to a UE, best channel assigned to UE with highest $G_{s,u}$
5: Let R_{min}^0 = minimum UE rate under this allocation
6: Let $\Phi^0 = E_s^0 + \alpha R_{min}^0$

Proposition 1. *Let* $(\Phi^* = E_s^* + \alpha R_{min}^*, A_s^*)$ *be the optimal solution of model (3.1), assume* $R_{min}^0 < R_{min}^*$*, let* $(\Phi^i = E_s^i + \alpha R_{min}^i, A_s^i)$ *be the solution of model (3.7), then* $\forall i, \Phi^i \leq \Phi^*$.

Proof. Because constraints (3.2, 3.3, 3.6, 3.5) in model (3.1) are the same as constraints (3.8, 3.9, 3.11, 3.12) in model (3.7), and $R_{min}^0 < R_{min}^*$, we must have A_s^* to be a candidate solution of model (3.7) and A_s^i to be a candidate solution of model (3.1). Assume $\exists \Phi^i$ such that $\Phi^i > \Phi^*$, then A^i is the optimal solution for model (3.1), which is contradictory to the assumption A^* is the optimal solution for model (3.1). □

Proposition 2. *Given a solution* $(A_s^{i-1}, E_s^{i-1}, R_{min}^{i-1})$ *of model (3.7), if* $R_{min}^{i-1} < R_{min}^*$ *and there is a feasible solution of model (3.7)* $(A_s^i, E_s^i, R_{min}^i)$*, then* $R_{min}^i \leq R_{min}^*$.

Proof. Assume $R_{min}^i > R_{min}^*$, if $E_s^i \geq E_s^*$, since $\Phi^i = E_s^i + \alpha R_{min}^i$, we have $\Phi^i > \Phi^*$. That is contradictory to proposition 1. If $E_s^i < E_s^*$, since A_s^* is also a candidate solution of model (3.7), which means E_s^i is not the maximum value. This violates (3.7), the objective function. Neither $E_s^i \geq E_s^*$ nor $E_s^i < E_s^*$ are valid, hence the assumption $R_{min}^i > R_{min}^*$ must be invalid. □

Proposition 3. *Given a solution* $(A_s^{i-1}, E_s^{i-1}, R_{min}^{i-1})$ *of model (3.7), if* $R_{min}^{i-1} < R_{min}^*$ *and there is no solution yields* R_{min} *such that* $R_{min}^{i-1} < R_{min} < R_{min}^*$*, then solving (3.7) will get the solution* $A_s^i = A_s^*$.

Proof. Because R_{min}^* is the next greater achievable minimum rate next to R_{min}^{i-1}, and A_s^* is also a candidate solution of (3.1), as per proposition 2, we must have $R_{min}^i = R_{min}^*$. Since A_s^* is the optimal solution for model (3.1), E_s^* is the maximum value given $R_{min} = R_{min}^*$. Hence $E_s^i = E_s^*$ and $A_{min}^i = A_{min}^*$. □

Proposition 3 indicates that starting from a low R_{min}^0, solving model (3.7) iteratively will find the optimal solution A_s^* along the way. A solution search algorithm 2 is proposed based on the propositions.

Algorithm 2 Solution Search Algorithm

1: feasible = True
2: **while** feasible **do**
3: solve model (3.7) with R_{min}^{i-1} by algorithm 3
4: **if** feasible solution found **then**
5: $R_{min}^{i} = \min(diag(A_s^{i\,T} R_s))$
6: $\Phi^i = E_s^i + \alpha R_{min}^i$
7: **if** $\Phi^i > \Phi^{i-1}$ **then**
8: $\hat{A}_s = A_s^i, \hat{R}_{min} = R_{min}^i, \hat{E}_s = E_s^i$
9: **end if**
10: $i = i + 1$
11: **else**
12: feasible = False
13: **end if**
14: **end while**

3.4.2 Model Linearization

Algorithm 2 solves (3.7) at step 3. However, (3.7) needs to be converted from the nonlinear objective function into a linear function first. If $y_0 = \frac{1}{\sum_c \sum_u a_{s,cu}}$, we change variables in the model as follows:

$$(3.7) \Rightarrow E_s^i = y_0 * \sum_c \sum_u a_{s,cu} r_{s,cu} \tag{3.13}$$

$$= \sum_c \sum_u (y_0 a_{s,cu}) r_{s,cu} \tag{3.14}$$

$$(3.8) \Rightarrow \sum_u a_{s,cu} \leq 1 \quad (u \in \{1..|U^s|\}) \tag{3.15}$$

$$\Rightarrow \sum_u a_{s,cu} y_0 \leq y_0 \tag{3.16}$$

$$\Rightarrow -y_0 + \sum_u a_{s,cu} y_0 \leq 0 \tag{3.17}$$

$$(3.9) \Rightarrow \sum_c a_{s,cu} \geq 1 \quad (c \in \{1..N\}) \tag{3.18}$$

$$\Rightarrow \sum_c a_{s,cu} y_0 \geq y_0 \tag{3.19}$$

$$\Rightarrow -y_0 + \sum_c a_{s,cu} y_0 \geq 0 \tag{3.20}$$

$$(3.10) \Rightarrow diag(A_s^T R_s) \succ \vec{\mathbb{1}} R_{min}^{i-1} \tag{3.21}$$

$$\Rightarrow \sum_c a_{s,cu} r_{s,cu} y_0 > R_{min}^{i-1} y_0 \tag{3.22}$$

$$\Rightarrow -y_0 R_{min}^{i-1} + \sum_c (a_{s,cu} y_0) r_{s,cu} > 0 \tag{3.23}$$

$$(3.11) \Rightarrow P_t \sum_c a_{s,cu} \leq P_{max} \quad (c \in \{1..N\}) \tag{3.24}$$

$$\Rightarrow P_t \sum_c a_{s,cu} y_0 \leq P_{max} y_0 \tag{3.25}$$

$$\Rightarrow -P_{max} y_0 + P_t \sum_c a_{s,cu} y_0 \leq 0 \tag{3.26}$$

We then define $y_{cu} = a_{s,cu} y_0$ and y_0 to be new variables. Relaxing the binary constraint (3.12) and substituting y_{cu} into Eq.(3.7, 3.8, 3.9, 3.10, 3.11), we obtain a transformed pure LP problem model as follows:

$$\mathbf{max}_{y_0, y_{cu}} \quad \sum_c \sum_u r_{s,cu} y_{cu} \tag{3.27}$$

$$\textbf{s.t.} \quad -y_0 + \sum_u y_{cu} \leq 0 \tag{3.28}$$

$$-y_0 + \sum_c y_{cu} \geq 0 \tag{3.29}$$

$$-y_0 R_{min}^{i-1} + \sum_c y_{cu} r_{s,cu} > 0 \tag{3.30}$$

$$-P_{max} y_0 + P_t \sum_c y_{cu} \leq 0 \tag{3.31}$$

$$y_{cu} \geq 0 \tag{3.32}$$

$$y_0 \geq 0 \tag{3.33}$$

$$\sum_{c}\sum_{u} y_{cu} = 1 \tag{3.34}$$

Model (3.27) is used in the Branch-Cut Algorithm (BCA) explained in the next section.

3.4.3 Solving by Branch-Cut Algorithm

We have followed the BCA procedure suggested in [Dim97, chapter 11] to solve our optimization problem. The BCA algorithm solving (3.7) includes the following steps: i) constraint relaxing, ii) branch and convert to pure LP problem and iii) update optimal solution or add cut into the loop to solve the problem. See algorithm 3 for the details.

At algorithm 3 step 12, since the optimal solution of the relaxed sub problem is smaller than the current best solution, there is no point to go further down the branch. For example, if the current sub problem is branched by adding c2: $a_{cu} = 0$ as a new constraint, and the relaxed sub problem solution is no better than the current optimal solution, then the algorithm adds cut $a_{cu} = 1$ as a new permanent constraint. Thus no additional sub problems would be branched out with $a_{cu} = 0$. This operation cuts the solver searching plan so that the solution could be found faster.

While algorithm 3 solves (3.7) iteratively, the overall optimization process sequentially solves model (3.7) until the problem becomes infeasible due to unachievable high minimum rate target. The optimization process may also stop in the event of an infeasible solution, or if the existing solution is satisfactory. By the time the process stops, the final solution is picked from the solution sequence as the solution with highest Φ.

3.5 Tracking ICI Dynamics

Optimization formulation (3.1) finds optimal channel allocation based on $I_{s,c}$ and CPV. Under the hood, the mechanism for this to work is that different BSs favor different channels by defining their CPV differently so that the ICI could be more likely avoided. However, as a distributed algorithm, there is no central coordinator that a BS can report CPV to and

Algorithm 3 Branch-Cut Algorithm

1: Deactivate constraint (3.12)
2: S_{optm} = minimum value
3: Select a variable $a_{s,cu}$ to generate two new constraints, c1: $a_{s,cu} = 1$; c2: $a_{s,cu} = 0$
4: Add the constraints back into the problem to create two sub problems, P(c1), P(c2)
5: Change variable on P(c1), P(c2) to obtain pure LP model as (3.27)
6: Solve sub problems to obtain optimal solution S^*_{sub} and Y^*, use Y^* to calculate A^*_s
7: **if** feasible solution is found **then**
8: **if** A^*_s is all integer **then**
9: Let $S_{optm} = S^*_{sub}, A^*_s = A^*_{sub}$ **if** $S_{optm} < S^*_{sub}$
10: **else**
11: **if** $S^*_{sub} < S_{optm}$ **then**
12: Add new constraint as cut to cut the branch
13: **else**
14: Pick arbitrary $A_s(c, u), (c \in C, u \in U)$ that is fractional number to repeat steps starting from 3
15: **end if**
16: **end if**
17: **else**
18: end and return no better solution found
19: **end if**

learn other BSs CPV from. A BS must figure that out by other means. A BS considers its environment, which consists of all its neighbor BSs, as a communication party that tries to tell the BS about its neighbors' CPV via ICI. Therefore, ICI can be considered as an information source. From the information source, a BS conjectures not only neighbors' CPV but whether they are undergoing significant change also called bifurcation in dynamical systems. A bifurcation means the system parameters have salient change. The change may be due to channel reallocation or UE mobility. This is critical to the success of channel allocation since updating CPV is superfluous if it is based on transient ICIPS fluctuation. Moreover, if not handled properly, it may make the ICIPS even more unpredictable to neighbor BS. This is the MDC problem we have mentioned earlier. To the best of our knowledge no distributed algorithm in the prior work has offered an effective solution for this. In this section, we explain our solution at microscopic and macroscopic levels in detail. At the microscopic level each channel ICI is estimated independently and system bifurcation is identified via ICI mutual information, whereas at the macroscopic level all channels' ICI is modeled as a ICIPS vector and tracked via phase point trajectory in the system phase space.

3.5.1 Microscopic level

ICI entropy definition Let $I_{s,c}$ denote the ICI level of channel c in BS s. Assuming $I_{s,c} \in [I_{c,min}, I_{c,max}]$, the range is divided into N' intervals. Both $I_{c,min}, I_{c,max}$ are algorithmic tunable parameters set by a heuristic method. In our simulation, the parameters are obtained from simulation runs without optimization on. In reality, both of them can be determined from historical field data logged by the BS. Let $I_{c,i} = (i + 0.5)I_r, (I_r = \frac{I_{c,max} - I_{c,min}}{N'}, i = 0, 1, 2, \cdots, N' - 1)$ denote the middle point of the ith interval. ICI probability distribution of channel c is denoted by $\pi_c = \{P_i | Prob(I_{s,c} \in [iI_r, (i + 1)I_r])\}$. A BS starts with a default π_c. It is also called BS' belief of the distribution, which should be updated whenever the channel ICI changes and $I_{s,c} = \sum_i P_i I_{c,i}$.

As $I_{s,c}$ reflects BS' belief on channel's ICI level, the entropy $H(\pi_c) = -\sum_{i=1}^{n} P_i log P_i$

tells how uncertain the belief is. Higher $H(\pi_c)$ more likely causes algorithm 3 performance degradation, since it depends on $I_{s,c}$.

System bifurcation and steadiness detection From the dynamical systems point of view, anything that has state variation can be regarded as a dynamical system. The system state is called phase, and state variation is modeled as a phase trajectory. A system's structural parameters change may be reflected in significant phase trajectory change. This is called system bifurcation. We view the channel ICI level as a dynamical system phase and attempt to identify the system bifurcation. The idea is to update BS' belief on channel ICI only between two consecutive bifurcations rather than a cross any of them.

In our study, the entire simulation running time is divided into periods. Each period has T (T $\gg N'$) time slots. For period t, T samples of $I_{s,c}$ are used to compute $\pi_{c,t}$. Assume X_t is a random variable, whose probability distribution is $\pi_{c,t}$. If the information source has not changed much, the random variables in the sequence $X_0, X_1, \ldots, X_{t-1}, X_t$ would have high correlation. From an information theory point of view, they carry information for each other. Let $H(X_t) = -\sum_{i=1}^{n} P_i^t log P_i^t$ be the entropy of X_t and $H(X_t|X_{t-1})$ be the conditional entropy between X_t and X_{t-1}. The mutual information of the sequence is defined as:

$$M_t^k = M(X_t; X_{t-1}, \ldots, X_{t-k}) \ \ (k \geq 1) \tag{3.35}$$

$$= H(X_t) - H(X_t|X_{t-1}, \ldots, X_{t-k}) \tag{3.36}$$

$$\text{if } M_t^k = 0 \Rightarrow H(X_t) = H(X_t|X_{t-1}, \ldots, X_{t-k}) \tag{3.37}$$

$$\Rightarrow X_{t-1}, \ldots, X_{t-k} \text{ carry no information of } X_t \tag{3.38}$$

The mutual information M_t^k is always non-negative and measures the dependence between the random variables. Eq. (3.38) shows that we would expect a drop in M_t^k, if the information source has significant change in the period that X_t samples. That's an indication of system bifurcation. Therefore, let M_{th} be the threshold that $M_t^k \geq M_{th}$ means information source is coherent or changed otherwise. The sequence length k in (3.35) is called the coherent period. When the information source is coherent, we consider the dynamical system to be steady.

ICI updating when the system is steady BS' belief on channels' ICI level is updated when the measured ICI is a sufficient distance away from the belief and the system is steady. The relative entropy $D(\pi_c//\pi_{c,t}) = \sum \pi_c log\frac{\pi_c}{\pi_{c,t}}$ is used to measure the distribution distance between current belief and current measurement. If D is too big, π_c needs an update and that is certainly conditional upon the environment steadiness. Algorithm 4 explains the whole procedure.

3.5.2 Dynamic CPV update algorithm

Once algorithm 4 detects channel ICI distribution change at step 11, instead of updating its belief right away, the algorithm starts a random length backoff timer. When the timer expires, algorithm 4 checks environment steadiness. If it is positive, channel $I_{s,c}$ is updated. The random backoff timer design is to prevent multiple BSs all seeing channel ICI varying in a steady environment and updating their belief of the same channel's ICI level simultaneously.

3.5.3 Macroscopic level

ICIPS tracking Section 3.5.1 describes the procedure for updating ICI probability distribution π_c for a single channel c. While each channel's ICI probability distribution is constantly updated independently, ICIPS needs to be properly tracked at the macroscopic level to avoid letting CPV follow the transient ICIPS readings. We model the ICIPS as a N-dimensional dynamical system, with N being the number of channels in a cellular sector s. We invent an imaginary particle phase point O_T^* to represent the current system phase, which is also the BS' belief on ICIPS. The subscript T denotes the time when BS' starts the belief. The O_T^*'s coordination is determined by a normalized ICIPS vector. Besides O_T^* we also create O_t, which gets updated on every time t and formally defined as follows:

$$I_{tot}^t = \sum_{c=1}^{N} I_{s,c}^t \tag{3.39}$$

$$P_{s,c}^t = \frac{I_{s,c}^t}{I_{tot}^t} \quad (c \in \{1..N\}) \tag{3.40}$$

Algorithm 4 Dynamic CPV Update Algorithm (DCUA)

steady = FALSE
$M_t^k = H(X_t) - H(X_t|X_{t-1}, \ldots, X_{t-k})$
if $M_t^k \geq M_{th}$ **then**
    k += 1
    if $k \geq N_k$ **then**
        steady = TRUE
    end if
else
    k = 1
end if
if $D(\pi_c//\pi_{c,t}) > D_{th}$ **then**
    if backoff_timer = 0 **then**
        backoff_timer = TM1
    else
        backoff_timer -= 1
    end if
    if backoff_timer = 0 **then**
        if steady = TRUE **then**
            $\pi_c = \pi_{c,t}$
            update $I_{s,c}$
        end if
    end if
else
    backoff_timer = 0
end if

$$O_t = \{P^t_{s,1}, P^t_{s,2}, \ldots, P^t_{s,N}\} \tag{3.41}$$

In the phase space, the two phase points O_t and O^*_T have their own trajectories. Like particles in the Newtonian world, the two phase points have imaginary force f between them. f constantly attracts O^*_T to meet with O_t. When that happens, the two phase points' trajectories merge and (O^*_T, T) is updated by (O_t, t). Before we give a formal definition of f, a few terms are defined as follows:

$$H^t_o = H(O_t) = -\sum_{c=1}^{N} P^t_{s,c} log P^t_{s,c} \tag{3.42}$$

$$H^*_o = H(O^*_T) = -\delta^{t-T} \sum_{c=1}^{N} P^*_{s,c} log P^*_{s,c} \quad (\delta > 1) \tag{3.43}$$

$$H_r = \frac{H^*_o}{H^t_o} \tag{3.44}$$

$$\Omega_t = D(O_t // O^*_t) \tag{3.45}$$

where Ω_t is the relative entropy of O_t and O^*_t, H^t_o is the entropy of O_t, H^*_o is the entropy of O^*_t scaled by a discount factor δ. The Eq. (3.43) shows H^*_o increases as time elapses. With all the terms defined, we give the formal definition of the dynamical system as follows:

$$f = \Omega_t H_r - \Omega_{th} \tag{3.46}$$

$$U(O_t) = \begin{cases} O^*_T & f \leq 0 \\ O_t & f > 0 \end{cases} \tag{3.47}$$

$$O^*_T = U(O_t) \tag{3.48}$$

where Ω_{th} is an algorithm defined threshold. Eq. (3.46) describes that f is first determined by the relative entropy Ω_t, which is the probability distribution distance between O_t and O^*_T. The bigger the distance between the two phase points the stronger f is. And then f is scaled by H_r. It is inversely proportional to H^t_o and proportional to H^*_o. The result

subtracts Ω_{th} and then Eq. (3.47) is used to determine whether O_T^* should move to meet with O_t.

CPV determination With the ICIPS properly tracked, we derive the CPV vector for BS s directly from O_T^* as $V_s = \{v_1, v_2, \ldots, v_N\} = \vec{\mathbb{1}} - O_T^*$. V_s is the complement of O_T^*. Let $D(V_s//V_{s'}) = \sum V_s log\frac{V_s}{V_{s'}}$ be the relative entropy between BS s and s', which measures how different V_s is from $V_{s'}$. While BS' distributively perform ICIPS tracking, we want the process to maximize $\sum_{s,s'} D(V_s//V_{s'}), (s, s'$ are any two adjacent BS). The larger the D is, the more likely BS may avoid ICI from neighbors effectively. CPV functions as a control variable. It extracts information from the environment and then impacts algorithm 3 behavior. The final goal is to let every BS in the same neighborhood favor different channels.

System convergence analysis When the algorithm starts, O_T^* is initialized to $O_T^* = \{\frac{1}{N}, \ldots, \frac{1}{N}\}, T = 0$, and then it gets updated via Eq. (3.47). In dynamical systems' language, x is called a fixed point if $S(x) = x$, where S is the system function. According to Eq. (3.47), O_t^* is at the fixed point. When f is not strong enough, $U(O_t)$ remains stable. As the indicator of environmental dynamics, when O_t deviates from O_T^*, Ω_t increases. The f is also controlled by the phase point uncertainty ratio H_r. The ratio amplifies the effect of Ω_t when the system has more uncertainty over O_T^* than O_t. The amplification effect makes the phase point to move even if Ω_t is small and turns the fixed point into a repellor. On the other hand, once the phase point settles at a position with low uncertainty, H_r has reduction effect on Ω_t. In the other words, O_t with relatively bigger Ω_t cannot attract O_t^* away from its original position. Hence that makes the fixed point an attractor. The δ discount factor in H_o^* starts to increase uncertainty after the phase point moves to a new position. Therefore we believe once O_t settles the O_T^* would finally be attracted to it.

3.5.4 Review and Heuristic Check

We have explained our optimization in previous sections. Figure 3.3 is included here to illustrate the dependence relationship between different key components used by the optimization

framework.

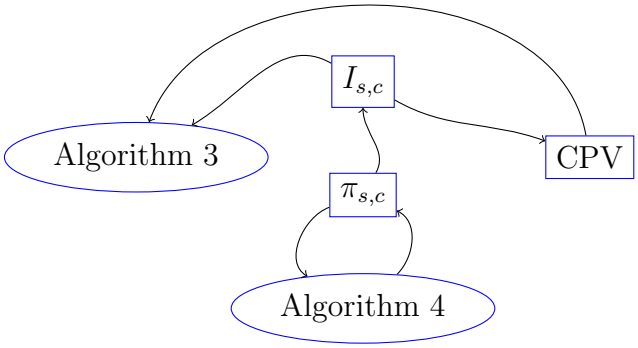

Figure 3.3: Optimization Key Components Dependency

Figure 3.3 shows that algorithm 4 monitors $\pi_{s,c}$ and updates it periodically. In turn, $I_{s,c}$ is directly derived from $\pi_{s,c}$. $I_{s,c}$ is used by algorithm 3 in its optimization and to compute CPV. Each arrow in the figure denotes a dependency relationship.

To verify our optimization methods heuristically, we first conducted a simplified scenario with only 3 BS' each adjacent to another. Each BS has 8 channels and 6 UEs. UEs are randomly located in the cell with no mobility. A brute force algorithm (BFA) is used to find the optimal solution. BFA knows all UE's TX power and locations across the mini network. It tries all the combinations of channel allocations and picks the one with the best spectral efficiency. Since proportional fairness (PF) is widely adopted in modern wireless cellular networks [LPM09, LRP17, KRS16], both DCUA-CPV and the PF algorithm are simulated in the mini network. In addition, we simulated the fair time-sharing RR algorithm suggested in [GFR18] for comparison. The mini network simulation runs for a limited period of time. The result shows that taking BFA performance as 100%, DCUA-CPV performance is around 86% and PF is 74%. The RR algorithm yields the poorest performance (61%) in this setup. Therefore, we will focus on analyzing DCUA-CPV and PF difference. The performance difference arises because the DCUA-CPV algorithm lets each cell gradually learn the neighbor cells channel allocation and adjust its own allocation to avoid ICI. On the other hand, the PF algorithm allocates channels based on whether a UE suffers from low traffic rate. Therefore, different BS may identify the same channel as a good channel and use

it. This increases the possibility of interference between BS. For large scale networks, BFA is not practical. It is however encouraging that our algorithm closes a significant fraction of the gap between the PF and BFA algorithms for this small example. In the next section, we will see that for larger scale networks the performance gain of DCUA-CPV over PF persists.

3.6 Simulation

3.6.1 Simulation Environment

3GPP RAN4 based Monte-Carlo static simulation is used as our simulation methodology [RSS10a]. We simulate both the USC and RSC OFDM networks described in section 3.3. Wrap-around is implemented for the USC network to tackle the network edge effect [RSS10a]. Each sector has 64 channels. UE locations in each sector are generated according to a uniformly random distribution. The radius is 1500 meters. The carrier frequency f_c is 2GHz. The total bandwidth is 100MHz. UE max transmission power is 23dBm. The urban macro-cell scenario in [P 08] is used for defining channel mode parameters. We use the channel propagation loss model defined in [P 08], which is a modified version of COST231-Hata model. Channel capacity is calculated by the Shannon channel capacity formula $C = Blog_2(1 + \frac{S}{N})$ [Gol05]. UEs that are close in location are likely to experience similar shadow fading. Therefore the WINNER II model requires shadow fading factor generated with correlation prorated to the distance between different UEs. We have implemented this feature in our simulation. By fine-tuning algorithms' parameters including $T, k, M_{th}, D_{th}, \alpha$ and backoff_timer used in the algorithms 3 and 4, we obtain simulation results explained in the next section.

3.6.2 Simulation Results and Discussions

Simulations are done for both low traffic loading, where the number of channels is greater than the number of UEs, and high traffic loading, in which they are the same. Our results include DCUA-CPV based and PF based channel allocation for comparison. Both RSC and

USC networks are simulated. Figure 3.4, 3.5 show the spectrum efficiency for different traffic loading cases in USC and RSC networks respectively.

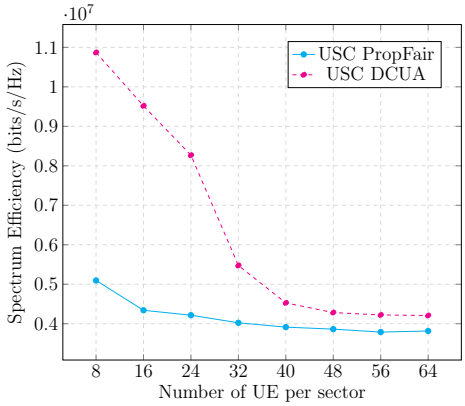

Figure 3.4: USC Spectrum Efficiency

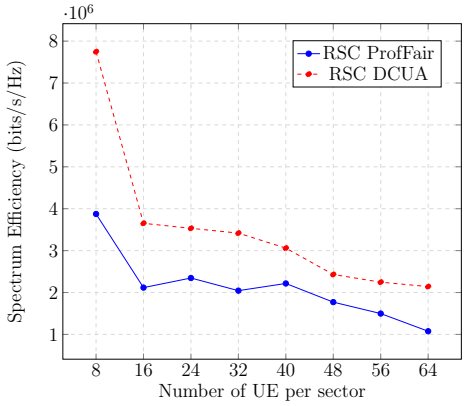

Figure 3.5: RSC Spectrum Efficiency

Our algorithm improves spectrum efficiency in all loading cases for both USC and RSC networks. The higher improvement in low loading cases is because there are more vacant channels for the algorithm to play with and adjacent sectors successfully avoid CPV collision. This inevitably reduces the effective ICI, which is defined to be the interference power seen in every transmission. In the high loading cases, since all UEs must be allocated channels for transmission and the number of UEs approaches the number of channels, even the channels with low CPV need to be used. The consequence is that more noisy channels will be used. That increases the bandwidth consumption but data throughput does not improve accordingly. Hence we see spectrum efficiency curve dropping in high loading area. As explained in

[LPM09], the PF based algorithm allocates channel resource according to the current channel quality indicator (CQI). However, the PF algorithm does not address the MDC problem inherent to multi-cell networks. Therefore, the CQI used in channel allocation may not be the same as that of run time especially in the high loading case. Our algorithm does a better job of keeping the channel quality indicator to be consistent from resource allocation decision time and the run time. Hence, we see our algorithm outperforms PF in terms of spectral efficiency. The improvement in minimum UE rate is shown in table 3.1.

Table 3.1: minimum UE rate

		USC		
Number of UE	8	16	24	32
PropFair	0.14256	0.019846	0.006356	0.0035705
DCUA-CPV	0.20354	0.029841	0.018349	0.0048620
Number of UE	40	48	56	64
PropFair	0.000923	0.000831	0.000781	0.000625
DCUA-CPV	0.001490	0.001503	0.001344	0.000727
		RSC		
Number of UE	8	16	24	32
PropFair	0.039676	0.016058	0.0061403	0.005144
DCUA-CPV	0.056284	0.019174	0.0091631	0.006898
Number of UE	40	48	56	64
PropFair	0.00514	0.00135	0.00402	0.00135
DCUA-CPV	0.00788	0.00317	0.00473	0.00154

In addition to Table 3.1, we include USC network UE rate variance results in figure 3.6. It is clear that DCUA-CPV algorithm results in a lower UE rate variance compared to PF.

The simulation results show that USC in general yields better performance than RSC. This is because RSC cells are randomly located. Cells close to each other generate much more ICI to each other compared to the USC case. For both USC and RSC, we see overall performance improves with our algorithm.

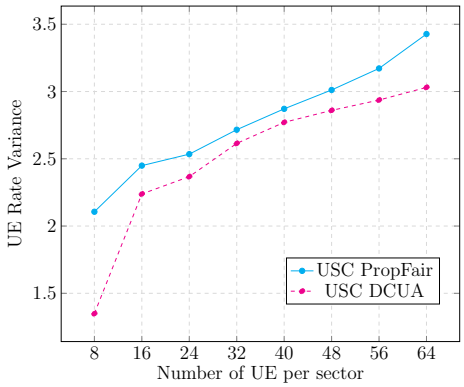

Figure 3.6: UE rate variance

3.7 Conclusion

We proposed a new optimization model to perform channel allocation for OFDMA networks. The algorithm has the merits of being autonomous and distributed with no inter-cell information exchange. It also resolves the inherent MDC issue for the non-centralized resource allocation algorithm. This is achieved by using an information theory based approach and a random backoff algorithm. We have shown that the algorithm successfully improves network spectrum efficiency and fairness in both USC and RSC networks.

For future research, we plan to incorporate power control into our optimization framework. We expect to see that by controlling UE TX power, the algorithm would have increased degrees of freedom for ICIPS tracking. In addition, this optimization framework should be a good fit to the resource allocation scenario including handoff, as the ICI fluctuation caused by UEs handoff is similar in nature to the dynamics we have already modeled.

CHAPTER 4

Optimizing Framework for Two-tier Network Handoff

4.1 Introduction

In the future heterogeneous network, network bandwidth and resource management faces new challenges and HO management is one of the most critical components to success. We need a new HO strategy because HO in the two-tier network has significant differences from the one tier counterpart. First, the HO performance is more sensitive to the UE mobility. This is because femto cell coverage is small, maybe fragmented, and HO policy has more options. Instead of just handover to a neighbor cell, in the two-tier network, UE may be handed over to a macro cell from a femto cell or vice versa. Selecting a macro or femto cell as the target BS has significant impact on HO performance. For example, a wrong decision may cause a ping-pong effect, which means the UE constantly performs HO between cells. Second, in comparison to the conventional received signal strength measurement based HO, there are more variables affecting HO and more parameters can be tuned to control HO. It would be rather difficult to construct a unified model to include all these variables. Finally, a two-tier network is usually deployed in urban areas, especially indoor environments with a high density of population. Wireless signals in this kind of environment are normally time varying and have high dynamics. It is challenging to implement optimization based on just received signal strength or distance to the BS. Moreover, unlike conventional single tier networks, target BS bandwidth availability should also be taken into account for HO. Otherwise, increasing blocking probability would jeopardize overall performance.

To tackle the challenges, we need a new methodology, which is flexible, simple and adaptive to the environment. To achieve this, we propose the following innovations: i)

A new optimization framework, which includes a HO algorithm to control the HO procedure and a machine learning (ML) algorithm to control the HO algorithm based on its historical observations. The two main components work in cooperation to create a flexible optimization design. In this design, every algorithm is replaceable. For example, there are many candidate machine learning algorithms. We use a modified version of the K-Nearest-Neighbor (KNN) algorithm here due to its simplicity. ii) A distance weight factor (DWF) algorithm that defines the way to calculate data point distance. iii) Weighted KNN algorithm. Unlike KNN algorithm that treats the K nearest neighbor opinions equally, WKNN takes disagreement within a group into account. The idea behind this approach is that we weight different opinions from different groups based on their uncertainty in their opinions. The uncertainty in opinion is measured by data points' disagreement, which is calculated as the average distance between them. In the other words, if the data points within a group are closer to one another, then its vote towards the group assignment of a new data point has more weight.

The approach introduced in this chapter is an enhancement of the conventional HO method. Unless the conventional HO algorithm is optimal, which is unlikely in the two-tier network scenario, there is room for improvement. From collected conventional HO performance data, a ML algorithm can identify the causality between the conditions and results and build up its knowledge accordingly. This is far beyond the capability of conventional HO algorithm using fixed or even adaptive thresholds. Fundamentally the ML algorithm is more knowledgeable because it mines more information from historical HO data. Moreover it only intervenes in the HO process when it believes there is a better decision. This provides a guarantee that it is always an enhancement.

In the rest of the chapter, we first revisit existing research work. Then we describe the system model used in this chapter. We then explain the framework in detail as well as WKNN and other algorithms. Finally, our simulation results are presented.

4.2 Related Work

The prior research on macro-femto heterogeneous network HO optimization can be categorized into several different approaches. A common one is to implement a learning algorithm or an inference engine of some sort as its core for making the HO decision. [NX15] suggests to use measured received signal strength indication (RSSI) of all neighbor cells at the HO scene as the location finger print. The algorithm learns causality between UE location represented by the finger print and HO performance, and uses that to make the HO decision. [CWX14] uses a Markov decision process (MDP) to model the HO decision and its consequence. The MDP defines call drop and switching cost as the penalty function, and data throughput as the reward function. A Q-learning algorithm is used to find the optimal policy. [KC15], [KLH17] both implement a fuzzy logic IF-THEN rule based inference engine in HO optimization.

The other common optimization practice is to construct a model to predict the next state of the UE to help HO. An optimized decision is made based on the prediction. [KLS15] proposes a time series model, logistic smooth threshold autoregressive (LSTAR) model, for SINR prediction, which is used by the target femto BS to prepare enough power for the incoming UE through HO. [CAL13] adds UE mobility direction prediction into the HO measurement report sent by the UE. The target BS uses the information for HO admission. [ZLX16] proposes to use a Gauss-Markov model for UE location and RSSI predictions. [QLT17] proposes a multi-objective optimization problem to predict and select the target BS to maximize achievable rate and reduce blocking probability.

The third approach employed by many researchers is to dynamically adjust various parameters to optimize the HO process in real time. [LCW16] proposes an algorithm to select a lightly loaded BS as the HO target BS. [GPZ16] divides the UE mobility trajectory into small time slots. A Markov process is created to model the UE state change and to estimate the HO time to trigger (TTT), which is dynamically adjusted to maximize the average performance. [HPH14] proposes an additional parameter, virtual offset for received signal strength (VORSS), to be used in HO. By dynamically adjusting VORSS, the HO algorithm

may control the selection of the HO target BS between the femto and macro cells. [BCN14] devises a sensing algorithm that derives cell preference value from BS RSSI and signal quality. The preference value is used to create a candidate target BS list. [ZXM14] proposes a hysteresis adjusting algorithm based on UE and BS distance. By dynamically updating hysteresis, the HO decision is optimized. [BRT14], [KK13] propose to use UE velocity and RSSI to form a prioritized HO list. UEs in the high priority list are likely to perform HO.

Besides the aforementioned HO optimization strategies, there are studies focusing on specific HO optimization aspects. [LP14b] proposes a Max-min based proportional fairness algorithm to achieve network load balancing via HO policy. [AK14], [DW13] and [THX13] all use auxiliary devices as helpers in HO. [AK14] creates a virtual BS out of all BS in the candidate list. [DW13] turns other UE into a device to device link to help on communication with neighbor cells. [THX13] proposes to dynamically expand home BS coverage to reduce the HO probability. [Fal13] proposes to divide UE links into call groups. Each group has different priority. During the HO, links with lower priorities may be dropped first to reduce the call drop probability. [LHN13] proposes a bandwidth limited HO admission policy to reduce HO block probability.

In our study, we offer an optimization framework, which is compatible to existing HO algorithms and adds a learning algorithm on top of it. Based on the collected statistical data, the learning algorithm is able to do optimization to further improve HO performance. As described in this section, prior works have optimized different quantitative metrics. Among them, we choose the ones that directly affect HO performance to form a multi-objective optimization. They include data throughput, HO ping-pong effect probability and radio link failure rate. We will explain the details in the next few sections.

4.3 System Model

We describe the system model in three aspects: network model, channel propagation model and user data traffic and mobility model.

Our study uses the scenario H1 described in [RSS10b] as the network model. The network

model is a two-tier multi-cell OFDMA network. It has one macro cell plus a 30 femto-cell network within it. The macro cell has 32 channels and the femto-cell has 10 channels. The femto-cell network is arranged in a 3 row flat layout to simulate one floor of an apartment complex. A user equipment (UE) may handover (HO) from the macro to the femto cell or vice versa.

We use the geometry based stochastic WINNER II channel model [P 08]. The channel model includes large scale (LS) and small scale (SS) parameters. The former includes parameters such as shadow fading. The latter includes parameters such as direction of arrival (DoA). WINNER II models correlations between LS parameters of two UE links towards the same BS. The correlation is proportional to the relative distance between the two UEs.

Poisson arrival models are used for the user traffic model. When the simulation starts the number of UEs for each cell is generated with a uniform distribution with its mean being a configurable simulation parameter. It remains constant during a simulation run. All UEs in the network have mobility with a *Smooth Random Mobility Model* (SRMM) described in [Bet01]. SRMM uses two stochastic processes for UE speed control and direction control. The speed control takes acceleration into account and changes incrementally. The direction change is also smooth. When a UE intends to turn, the direction is changed in several time steps until the new target direction is achieved. Both stochastic processes include parameters that can be tuned to model different mobility behaviors including pedestrian and vehicle.

4.4 Optimizing Framework

4.4.1 Optimization Goal and Three-tier Framework

The framework targets a multi-objective optimization goal. This includes network data throughput improvement (D), ping-pong effect rate (P) reduction and radio link failure rate reduction (F). The optimization goal is:

$$\textbf{min} \;\; \alpha_1 \frac{1}{D} + \alpha_2 F + \alpha_3 P \tag{4.1}$$

where $\alpha_1, \alpha_2, \alpha_3$ are weight factors.

To optimize the HO against the goal, our approach is to use the existing HO algorithm as the basic HO procedure and make improvements on top of it. While the basic HO procedure runs, HO information is collected. The HO optimization algorithm analyzes the collected information and may override the HO decision made by the basic procedure when it believes that it has a better one. Since the optimization relies on an existing HO algorithm and always tries to do better when it builds enough confidence in the decision, we can reasonably expect that the optimization will improve HO performance unless the basic HO procedure always makes optimal decisions.

In theory, the candidate for the basic HO procedure can be any HO algorithm. In our study, we use the Third Generation Partnership Project (3GPP) HO procedure explained in [LCW16] and [AMY14] as the basic HO procedure. We implement a three-tier optimization framework. It is run by every BS. The HOC in the lower tier runs the 3GPP HO procedure. Information regarding each performed HO is used to generate a HO data sample. The HOC feeds HO data samples into the DSS, which runs in the upper tier of the framework. The DSS then runs a selection algorithm to save the selected data samples into the TDS. The LA in the middle tier runs a machine learning algorithm, KNN in our study, over the TDS to determine various optimization parameters. When the LA is confident that it has a better solution than the basic HO algorithm, it sends a command to the HOC to make the correction. Figure 4.1 shows the framework structure.

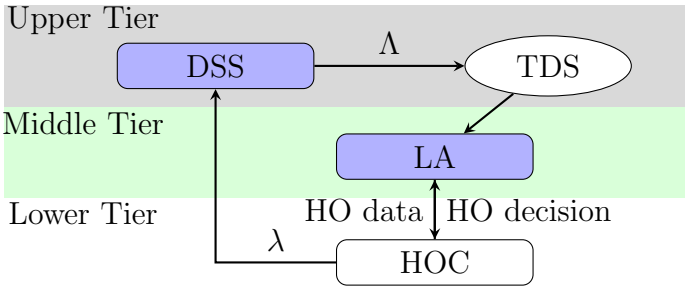

Figure 4.1: HO Optimization Framework

The entire framework can be seen as a closed-loop control system with a feedback route.

The following sections explain each component in detail.

4.4.2 Upper Tier Operation

Data sample definition Let $\lambda = \{\vec{\gamma}, B_\delta\}$, where $\vec{\gamma}$ denotes the neighbor BS' (including target BS) SINR vector measured before the HO decision was made and B_δ be the payoff value of handover to target BS δ. The payoff value denotes the HO performance result calculated according to Eq. (4.1) by the HOC. λ is fed by the HOC to DSS and is considered as the raw HO data collected directly from HO operation.

Let $\Lambda = \{\vec{\psi}, \vec{\nu}, \gamma, \rho, B_\delta\}$ be a derived HO data sample vector. $\vec{\psi}$ denotes the UE location; $\vec{\nu}$ denotes the UE mobility vector. Both $\vec{\psi}, \vec{\nu}$ are derived terms that will be explained in the next section. ρ is the max available vacant channel preference value (CPV) in the target BS. CPV is a channel resource allocation metric used by every BS for its uplink channel. Assuming there are N uplink channels for each BS, let I_c be the interference level on channel c. CPV for channel c is defined as $v_c = \frac{\sum_{i=1}^{N} I_i}{I_c H_c}$, where $H_c = -\sum_{i=1}^{n} P_i log P_i$ (P_i is the probability of channel interference level in interval i) is the entropy of I_c. The H_c determines how uncertain the BS sees I_c on channel c. The higher and more uncertain I_c is, the lower v_c would be. ρ is an indicator of channel quality and availability in the target BS. It is defined as $\arg\max_c \rho = \{v_c | \text{channel } c \text{ is vacant}\}$.

Data Sample Selector The DSS has two major responsibilities including converting λ to Λ and selectively forwarding Λ to the TDS.

The DSS first augments λ by adding two derived terms $\vec{\psi}$ and $\vec{\nu}$. $\vec{\psi}$ is UE's location obtained using its measured neighbor BS' received signal strength vector. This will usually be a good approximation because we can reasonably assume a BS' received signal strength level seen by an UE is highly correlated with the distance between them. Since BS' location is known, by checking signal strength from different neighbor BS, DSS derives an estimation of the UE's location.

The other derived term $\vec{\nu}$ is calculated by DSS using UE's historical λ data. By checking

$\vec{\gamma}$ fluctuation level in a unit time interval, the DSS estimates the fading level of the UE and the velocity of the UE. Next the DSS estimates the moving direction by computing the difference of two consecutive locations of the UE.

Then the DSS only keeps the HO target BS' received signal strength γ from $\vec{\gamma}$ and together with $\vec{\psi}, \vec{\nu}$ to generate Λ. Next the DSS selects the data points by their payoff value B_δ and aims at picking up HO data samples with performance results better than threshold (ζ). Each BS maintains a HO data sample set TDS to store HO data samples H_i^b, where b is the target BS and i is the index of the data sample. Algorithm 5 explains the details. The algorithm first checks whether the new data samples fall into the coherent period (τ) of any previous HO data samples for the same UE. This is necessary for ping-pong effect calculation, since if a ping-pong effect happens to a UE, the selector would see a sequence of HO data. If the interval between two HO data samples of the same UE is beyond τ, the latter HO is considered to be a brand new HO event.

4.4.3 Middle Tier Operation

Data sample distance As described in the previous section, HO data samples are organized per their handover targeted BS b in TDS, denoted as TDS_b. The distance between any two data points $\{H_i^b, H_j^b\} \in TDS_b$ is defined as $d_{i,j}^b(\vec{w}) = w_0 d_{\psi,i,j}^b + w_1 d_{\nu,i,j}^b + w_2 d_{\gamma,i,j}^b + w_3 d_{\rho,i,j}^b$, where $\vec{w} = (w_0, w_1, w_2, w_3)^T$ is the distance weight vector, $d_\psi^b = \left\| \vec{\psi_i^b} - \vec{\psi_j^b} \right\|$ is the Euclidean distance between the two HO locations; $d_\nu^b = \left\| \vec{\nu_i^b} - \vec{\nu_j^b} \right\|$ is the distance between the mobility vectors; $d_\gamma^b = \gamma_i^b - \gamma_j^b$; $d_\rho^b = \rho_i^b - \rho_j^b$. We also define target BS total data sample distance as $D^b = \sum_{i=1}^{K-1} \sum_{j=i+1}^{K} d_{i,j}^b$, where $K = |TDS_b|$.

Distance weight vector Whenever TDS is updated with new data samples, the weight factor $\vec{w}$ is optimally determined. The optimization goal is to minimize the total distance among all data samples in TDS. In the other words, data samples leading to a similar HO decision should be close to each other in distance. With the definitions in the section 4.4.3, we derive:

Algorithm 5 DSS algorithm

compute $\vec{\psi}$ from $\vec{\gamma}$
compute $\vec{\nu}$ from $\vec{\gamma}$ and $\vec{\psi}$
receive $H^b_{u,t} = \Lambda$ for UE u at time t
if there exists an $H^{b'}_{u,t'}$ saved before at t' **then**
  if $(t - t') > \tau$ **then**
    if $H^b_{u,t}(B_\delta) > \zeta$ **then**
      save $H^b_{u,t}$ into TDS as a new data sample
    end if
  else
    update $H^{b'}_{u,t'}(B_\delta)$
    let $t' = t$
  end if
else
  if $H^b_{u,t}(B_\delta) > \zeta$ **then**
    save $H^b_{u,t}$ into TDS as a new data sample
  end if
end if

$$D^b = \sum_{i=1}^{K-1} \sum_{j=i+1}^{K} d^b_{i,j}(\vec{w}) \tag{4.2}$$

$$= \sum_{i=1}^{K-1} \sum_{j=i+1}^{K} (w_0 d^b_{\psi,i,j} + w_1 d^b_{\nu,i,j} + w_2 d^b_{\gamma,i,j} + w_3 d^b_{\rho,i,j}) \tag{4.3}$$

$$= w_0 \sum_{i=1}^{K-1} \sum_{j=i+1}^{K} d^b_{\psi,i,j} + w_1 \sum_{i=1}^{K-1} \sum_{j=i+1}^{K} d^b_{\nu,i,j} + w_2 \sum_{i=1}^{K-1} \sum_{j=i+1}^{K} d^b_{\gamma,i,j} + w_3 \sum_{i=1}^{K-1} \sum_{j=i+1}^{K} d^b_{\rho,i,j} \tag{4.4}$$

$$= w_0 D^b_0 + w_1 D^b_1 + w_2 D^b_2 + w_3 D^b_3 \tag{4.5}$$

where D^b_0, D^b_1, D^b_2 and D^b_3 replace the corresponding terms in Eq.(4.4). The total distance

can be defined as

$$\sum_{b\in B} D^b = w_0 \sum_{b\in B} D_0^b + w_1 \sum_{b\in B} D_1^b + w_2 \sum_{b\in B} D_2^b + w_3 \sum_{b\in B} D_3^b \tag{4.6}$$

$$= w_0 D_0^B + w_1 D_1^B + w_2 D_2^B + w_3 D_3^B \tag{4.7}$$

where B denotes the data sample set for target BS B. We have a distance determination model as follows:

$$\min_{\vec{w}} \quad w_0 D_0^B + w_1 D_1^B + w_2 D_2^B + w_3 D_3^B \tag{4.8}$$

$$\textbf{s.t.} \quad \vec{\mathbb{1}}^T \vec{w} = 1 \tag{4.9}$$

$$\vec{w} \succeq 0 \tag{4.10}$$

Eq.(4.8) is a linear programming problem. By the constraints (4.9) and (4.10), $\vec{w}$ can be regarded as a probability distribution. To calculate the optimal value of Eq.(4.8), we simply allocate all the probability to the minimum D_i^B. To prove this, let $I_m = \{i | D_i^B = d_{min}, i = 0..3\}$, where d_{min} is the minimum value of all coefficients.

$$P_w = \sum_{i\in I_m} w_i \tag{4.11}$$

$$S_m = \sum_{i\in I_m} D_i^B w_i \tag{4.12}$$

$$= d_{min} \sum_{i\in I_m} w_i = d_{min} P_w \tag{4.13}$$

Let $J = \bar{I_m}$, if $P_w < 1$, then we obtain,

$$(4.8) = d_{min} P_w + D_j^B (1 - P_w) \quad j \in J \tag{4.14}$$

$$\because D_j^B > d_{min} \tag{4.15}$$

$$\therefore (4.8) > d_{min}P_w + d_{min}(1 - P_w) \tag{4.16}$$

$$= S_m \tag{4.17}$$

Based on the conclusion, we devise the distance weight factor (DWF) algorithm

Algorithm 6 DWF algorithm

1: $d_{min} = min(D_i^B),\ i = 0..3$

2: $w_i = \frac{1}{|I_m|},\ i \in I_m$

3: $w_j = 0,\ j \in J$

Weighted KNN learning The LA is the core in the middle tier of the framework. We propose the weighted K-Nearest-Neighbor (KNN) algorithm for the LA. Traditional KNN determines to which group the new data sample belongs to by taking votes from K nearest neighbors in distance.

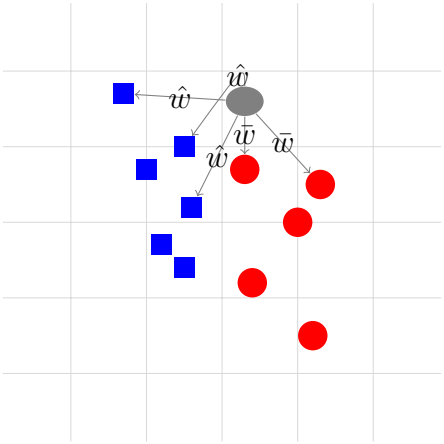

Figure 4.2: K=5 nearest neighbor classifier with weight

In our study, we do not consider every neighbor data sample with equal weight. Figure 4.2 is an example for weighted KNN. The ellipse data point consults its 5 nearest neighbors to determine whether it belongs to the circle or the square group. However, the circle and square data samples are evaluated with weights of $\bar{w}, \hat{w}$ respectively. In our study, we determine the weight by data uncertainty. The uncertainty is measured by the disagreement (average distance) between the data samples in the group of the same target BS. Let w^b be

the weight for data samples with HO target BS b, B be the set of all BS, $w^b = \frac{D^b}{\sum_{b' \in B} D^{b'}}$. Let $HO(b)$ be the HO decision, $K(b)$ be the set of BS the selected K data samples have. We obtain

$$HO(b) = \underset{b}{\mathbf{argmax}} |K(b)| w^b \tag{4.18}$$

Algorithm 7 realizes Eq.(4.18)

Algorithm 7 Weighted KNN Learning Algorithm

1: Select K nearest neighbors of data samples
2: **for** $b \in K(b)$ **do**
3: calculate $|K(b)|w^b$
4: **end for**
5: return the BS that has max $|K(b)|w^b$

4.4.4 HO Controller

The HOC operates in the lower tier of the framework. By default it runs the UE HO operation to comply to 3GPP. When a UE meets the standard 3GPP HO criteria, the HOC forwards its data to the LA. The LA may override the default HO decision, if it thinks a better HO decision could be made based on its knowledge. Once a HO operation is done, the HOC keeps track of the UE and collects its post HO performance report. A HO data sample is generated by combining the HO status and performance report. The HOC then feeds the data to the DSS in the upper tier.

4.5 Simulation

4.5.1 Simulation Environment

Monte-Carlo static simulation is used as our simulation methodology [RSS10b]. The carrier frequency f_c is 2GHz. The total bandwidth is 100MHz. UE max transmission power is

23dBm. The urban macro-cell scenario in [P 08] is used for defining channel mode parameters. The channel propagation loss is computed as: $PL = PL_{free} + SF + AG, PL_{free} = 20log_{10}(d) + 46.4 + 20log_{10}(\frac{f_c}{5})$, where d is the distance between UE and BS antenna. Channel capacity is calculated by the Shannon channel capacity formula $C = Blog_2(1 + \frac{S}{N})$ [Gol05]. AG is the antenna gain calculated using azimuth antenna pattern. SF is the shadow fading factor. It is a random variable with a Gaussian distribution. Its standard deviation is 4. UEs that are close in location are likely to experience similar shadow fading. Therefore the WINNER II model requires SF generated with correlation prorated to the distance between different UEs. We have implemented this feature in our simulation. We obtain simulation results explained in the next section.

4.5.2 Simulation Results and Discussion

Simulations are done for setting different average UE speeds into the mobility model proposed in [Bet01]. The 3GPP standard HO procedure is simulated for comparison. Figure 4.3 shows the network overall data throughput results. We see that our algorithm yields a much better performance. This is a result of multiple factors. First of all, each BS keeps track of channel noise level by CPV. High CPV indicates the channel is less noisy. The max available vacant channel CPV ρ is taken into account by the optimization algorithm, so it makes it more likely that a UE handovers to a target BS with a cleaner channel. This effect improves data link throughput.

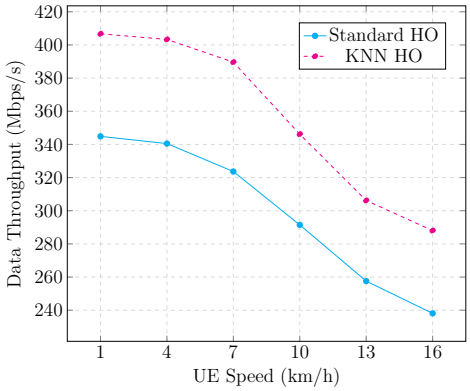

Figure 4.3: Network Data Throughput

Secondly, the optimization aims at ping-pong effect reduction. As shown in figure 4.4, our optimization significantly reduces the ping-pong HO probability. The LA in the optimization learns what kind of HO data sample is likely to cause ping-pong HO from the historical data in TDS and tries to avoid them. Reduction in unnecessary HOs reduces the data link interruption time and improves data throughput.

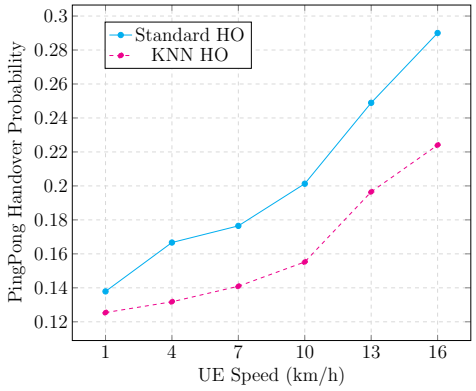

Figure 4.4: PingPong HO Probability

Figure 4.5 shows that our optimization has noticeable reduction in link failure probability. It is expected that greater UE speed causes higher probability of link drop. By taking mobility into account in the HO decision, the optimization improves the performance in this regard either by handover of the UE to the macro BS or by finding a better femto BS along the mobility direction instead of the current BS with better signal strength. Thus, the proposed framework can improve the performance with respect to all three goals.

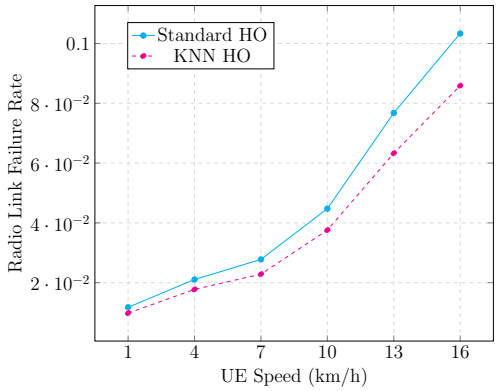

Figure 4.5: Call Failure Probability

4.6 Conclusion

We proposed a new optimization framework to perform HO management in macro-femto cell heterogeneous networks. The framework has the merit of being flexible as it may accommodate any basic HO algorithms, which interfaces with the upper level machine learning algorithm for further performance improvement. Not only can the algorithm components be replaced, but the threshold conditions for overriding the basic HO algorithm decision can be fine tuned. In this chapter, we proposed a WKNN algorithm for the machine learning algorithm in the framework. The WKNN algorithm improves in data point classification performance by properly weighting neighbors. We have shown that the optimization successfully improves HO performance against the given multi-objective target in the heterogeneous network.

Given the fact that macro and femto cells may work on different frequencies, the propagation model needs to account for additional variables. This makes the need for a machine learning algorithm to deal with the variation is even stronger, along with the notion of having possibly multiple base HO algorithms that the supervisory ML layer selects. Hence, we suggest future study in this direction.

CHAPTER 5

Concluding Remarks

In this work we propose an optimization framework for OFDMA network channel resource allocation and UE handover management. The optimization framework has been proven to work with USC and RSC networks as well as macro, femto two-tier heterogeneous networks. The 2-dimensional and two-tier network optimization is a complex problem due to traffic loading variation, UE mobility and environment dynamics. Among all the difficulties, the MDC problem is the hardest one to overcome. However, we have successfully solved these problems in our proposed optimization framework.

First, we studied the channel resource allocation optimization problem in the macro cell network. The goal is to improve the network traffic throughput and at the same time maintain fairness between UEs. We identified that ICI avoidance is one of the major challenges in channel resource allocation. This is associated with the MDC problem, which makes it even harder to resolve. In this work, we defined the multi-objective optimization formulation and then reformulated it into a simplified LP model. The optimization algorithm sequentially solves the LP model to approach the optimal solution of the original model. To tackle the MDC problem, we treat the ICI as an information source and determine the environmental steadiness via mutual information of ICI. The framework includes all these optimization algorithms to enable every cell to perform channel allocation and ICI avoidance distributively. Our simulation result shows the algorithm works well.

Next, we studied the macro-femto two-tier network handover problem. We proposed an multi-tier optimization framework to combine handover algorithm with a LA, which can be realized by different machine learning algorithms. The idea behind this can be summarized into a few points:

1. Different HO execution algorithms can be used and operation data is collected
2. LA may use different machine learning algorithms
3. LA studies data and issues its own judgement to override HO execution algorithm's decision when necessary

With this setup, the HO execution algorithm knows the operation, while LA has the intelligence. While flexibility is an obvious advantage of the framework, it is also adaptive to the environment and distributed. In this work, we propose a modified version of the KNN algorithm, WKNN, to be the core algorithm of LA. WKNN not only studies neighbor's vote on decisions but the degree of disagreement in different group's members as well. However, any appropriate machine learning algorithm can be used. Using a machine learning technique in handover has another important merit. From the optimization point of view, the differences between how to treat macro and femto cells is learned by the LA. In the other words, LA may not be aware a macro or femto cell is involved in the operation. All it sees are data samples. The fact that the LA makes different HO decision is equivalent to HO parameter customization for different scenarios. However, the customization is done by the LA automatically instead of the algorithm designer.

Finally, the channel resource allocation and handover optimization meet at incorporating cell channel allocation consideration into handover optimization framework. In this thesis, we have proposed a distributed channel allocation algorithm using CPV. While each BS allocating its own channel independently with no explicit information exchange can be an advantage, BS' connect to each other when a UE handovers from one to the other. We consider the HO optimization framework to be a higher level framework, which is more generic than the channel allocation optimization framework. Thus the latter can be integrated very well into the former. In reality, since there is signaling message exchange during the HO procedure, different BS' CPV state information can be propagated via those signaling messages. Therefore this information can be utilized by the LA in the HO optimization framework to not only determine target BS' resource availability but also help in BS received signal strength measurement predication as well. Extending the multi-tier approach to the

channel assignment problem within cells or indeed to any resource allocation problem in radio would be a very interesting question for follow on research.

Our simulation shows the proposed algorithm successfully optimized handover performance compared to a traditional basic handover algorithm. By studying different scenarios, the optimization framework shows promising improvements over other proposed methods. An interesting future work could be to incorporate power control as another dimension into the framework and expand the handover decision space to include more parameters for the LA.

REFERENCES

[AK14] M. Ahmed and J. Kim. "Context aware network-assisted hand-off management and interference mitigation scheme for heterogeneous networks." In *2014 IEEE Wireless Communications and Networking Conference (WCNC)*, pp. 2970–2975, April 2014.

[AMY14] O. Altrad, S. Muhaidat, and P. D. Yoo. "Doppler frequency estimation-based handover algorithm for long-term evolution networks." *IET Networks*, **3**(2):88–96, June 2014.

[Ash90] Robert B. Ash. *Information theory*. Dover Publications, Inc., 31 East 2nd Street, Mineola, N.Y. 11501, 1 edition, 1990.

[BCN14] M. Behjati, J. P. Cosmas, R. Nilavalan, G. Araniti, and M. Condoluci. "Self-organising comprehensive handover strategy for multi-tier LTE-Advanced heterogeneous networks." *IET Science, Measurement Technology*, **8**(6):441–451, 2014.

[Bet01] Christian Bettstetter. "Mobility Modeling in Wireless Networks: Categorization, Smooth Movement, and Border Effects." *SIGMOBILE Mob. Comput. Commun. Rev.*, **5**(3):55–66, July 2001.

[BRT14] M. Boujelben, S. Ben Rejeb, and S. Tabbane. "A novel self-organizing scheme for 4G advanced networks and beyond." In *Networks, Computers and Communications, The 2014 International Symposium on*, pp. 1–5, June 2014.

[CAL13] A. Ben Cheikh, M. Ayari, R. Langar, G. Pujolle, and L. A. Saidane. "Optimized handover algorithm for two-tier macro-femto cellular LTE networks." In *2013 IEEE 9th International Conference on Wireless and Mobile Computing, Networking and Communications (WiMob)*, pp. 608–613, Oct 2013.

[CWX14] X. Chen, H. Wang, X. Xiang, and C. Gao. "Joint handover decision and channel allocation for LTE-A femtocell networks." In *Game Theory for Networks (GAMENETS), 2014 5th International Conference on*, pp. 1–5, Nov 2014.

[CWZ12] J. Chen, P. Wang, and J. Zhang. "Adaptive soft frequency reuse scheme for inbuilding dense femtocell networks." In *2012 1st IEEE International Conference on Communications in China (ICCC)*, pp. 530–534, Aug 2012.

[Dim97] John N. Tsitsiklis Dimitris Bertsimas. *Introduction to Linear Optimization*. Athena Scientific, PO Box 391, Belmont, Mass. 02178-9998 USA, 1 edition, 1997.

[DW13] U. Dampage and C. B. Wavegedara. "A low-latency and energy efficient forward handover scheme for LTE-femtocell networks." In *2013 IEEE 8th International Conference on Industrial and Information Systems*, pp. 53–58, Dec 2013.

[Fal13] O. E. Falowo. "Selective call-dropping and bandwidth adaptation for reducing multiple-call handoff dropping." In *2013 IEEE Globecom Workshops (GC Wkshps)*, pp. 958–962, Dec 2013.

[GBA12] R.K. Ganti, F. Baccelli, and J.G. Andrews. "Series Expansion for Interference in Wireless Networks." *Information Theory, IEEE Transactions on*, **58**(4):2194–2205, 2012.

[GFR18] J. Garca-Morales, G. Femenias, and F. Riera-Palou. "On the Design of OFDMA-Based FFR-Aided Irregular Cellular Networks With Shadowing." *IEEE Access*, **6**:7641–7653, 2018.

[GH09] R.K. Ganti and M. Haenggi. "Interference and Outage in Clustered Wireless Ad Hoc Networks." *Information Theory, IEEE Transactions on*, **55**(9):4067–4086, 2009.

[Gol05] Andrea Goldsmith. *Wireless communications*. Cambridge University Press, 32 Avenue of the Americas, New York, NY 10013-2473, USA, 3 edition, 2005.

[GPZ16] F. Guidolin, I. Pappalardo, A. Zanella, and M. Zorzi. "Context-Aware Handover Policies in HetNets." *IEEE Transactions on Wireless Communications*, **15**(3):1895–1906, March 2016.

[HKH13] A. Hamza, S. Khalifa, H. Hamza, and K. Elsayed. "A Survey on Inter-Cell Interference Coordination Techniques in OFDMA-Based Cellular Networks.", 2013.

[HL14] V. Nguyen Ha and L. Bao Le. "Fair Resource Allocation for OFDMA Femtocell Networks With Macrocell Protection." *IEEE Transactions on Vehicular Technology*, **63**(3):1388–1401, March 2014.

[HPH14] M. S. Hung, J. Y. Pan, and Z. E. Huang. "Analysis of Handover Decision with Adaptive Offset in Next-Generation Hybrid Macro/Femto-cell Networks." In *Intelligent Information Hiding and Multimedia Signal Processing (IIH-MSP), 2014 Tenth International Conference on*, pp. 729–734, Aug 2014.

[KC15] I. Kustiawan and K. H. Chi. "Handoff Decision Using a Kalman Filter and Fuzzy Logic in Heterogeneous Wireless Networks." *IEEE Communications Letters*, **19**(12):2258–2261, Dec 2015.

[KHK05] Keunyoung Kim, Youngnam Han, and Seong-Lyun Kim. "Joint subcarrier and power allocation in uplink OFDMA systems." *IEEE Communications Letters*, **9**(6):526–528, Jun 2005.

[KK13] W. Khalid and K. S. Kwak. "Handover optimization in femtocell networks." In *2013 International Conference on ICT Convergence (ICTC)*, pp. 122–127, Oct 2013.

[KKL15] S. Y. Kim, J. A. Kwon, and J. W. Lee. "Sum-Rate Maximization for Multicell OFDMA Systems." *IEEE Transactions on Vehicular Technology*, **64**(9):4158–4169, Sept 2015.

[KLH17] I. Kustiawan, C. Y. Liu, and D. F. Hsu. "Vertical Handoff Decision Using Fuzzification and Combinatorial Fusion." *IEEE Communications Letters*, **21**(9):2089–2092, Sept 2017.

[KLS15] S. Kabiri, T. Lotfollahzadeh, M. G. Shayesteh, and H. Kalbkhani. "Modelling and forecasting of signal-to-interference plus noise ratio in femtocellular networks using logistic smooth threshold autoregressive model." *IET Signal Processing*, **9**(1):48–59, 2015.

[KN00] I. Katzela and M. Naghshineh. "Channel assignment schemes for cellular mobile telecommunication systems: A comprehensive survey." *Communications Surveys Tutorials, IEEE*, **3**(2):10–31, 2000.

[KNH17] M. Kaneko, T. Nakano, K. Hayashi, T. Kamenosono, and H. Sakai. "Distributed Resource Allocation With Local CSI Overhearing and Scheduling Prediction for OFDMA Heterogeneous Networks." *IEEE Transactions on Vehicular Technology*, **66**(2):1186–1199, Feb 2017.

[KRS16] B. Khamidehi, A. Rahmati, and M. Sabbaghian. "Joint Sub-Channel Assignment and Power Allocation in Heterogeneous Networks: An Efficient Optimization Method." *IEEE Communications Letters*, **20**(12):2490–2493, Dec 2016.

[LCB12] Jingya Li, Xin Chen, C. Botella, T. Svensson, and T. Eriksson. "Resource allocation for OFDMA systems with multi-cell joint transmission." In *Signal Processing Advances in Wireless Communications (SPAWC), 2012 IEEE 13th International Workshop on*, pp. 179–183, 2012.

[LCK08] Zhenyu Liang, Y.H. Chew, and Chi Chung Ko. "Decentralized bit, subcarrier and power allocation with interference avoidance in multicell OFDMA systems using game theoretic approach." In *Military Communications Conference, 2008. MILCOM 2008. IEEE*, pp. 1–7, 2008.

[LCS12] Quang Duy La, Yong Huat Chew, and Boon Hee Soong. "Performance Analysis of Downlink Multi-Cell OFDMA Systems Based on Potential Game." *Wireless Communications, IEEE Transactions on*, **11**(9):3358–3367, 2012.

[LCW16] Y. Li, B. Cao, and C. Wang. "Handover schemes in heterogeneous LTE networks: challenges and opportunities." *IEEE Wireless Communications*, **23**(2):112–117, April 2016.

[LHN13] L. B. Le, E. Hossain, D. Niyato, and D. I. Kim. "Mobility-aware admission control with QoS guarantees in OFDMA femtocell networks." In *2013 IEEE International Conference on Communications (ICC)*, pp. 2217–2222, June 2013.

[LL05] G. Li and H. Liu. "On the optimality of the OFDMA network." *IEEE Communications Letters*, **9**(5):438–440, May 2005.

[LP14a] W. Li and G. Pottie. "Fair resource allocation for OFDMA multi-cell networks." In *Information Theory and Applications Workshop (ITA), 2014*, pp. 1–7, Feb 2014.

[LP14b] P. M. Fei Liu and M. Petrova. "A handover scheme towards downlink traffic load balance in heterogeneous cellular networks." In *2014 IEEE International Conference on Communications (ICC)*, pp. 4875–4880, June 2014.

[LPM09] S. B. Lee, I. Pefkianakis, A. Meyerson, S. Xu, and S. Lu. "Proportional Fair Frequency-Domain Packet Scheduling for 3GPP LTE Uplink." In *IEEE INFOCOM 2009*, pp. 2611–2615, April 2009.

[LRP17] F. Liu, J. Riihijrvi, and M. Petrova. "Analysis of Proportional Fair Scheduling Under Bursty On-Off Traffic." *IEEE Communications Letters*, **21**(5):1175–1178, May 2017.

[MAP16] N. Mokari, F. Alavi, S. Parsaeefard, and T. Le-Ngoc. "Limited-Feedback Resource Allocation in Heterogeneous Cellular Networks." *IEEE Transactions on Vehicular Technology*, **65**(4):2509–2521, April 2016.

[MNM16] M. Mostafavi, J. M. Niya, H. Mohammadi, and B. M. Tazehkand. "Fast convergence resource allocation in IEEE 802.16 OFDMA systems with minimum rate guarantee." *China Communications*, **13**(12):120–131, December 2016.

[MTB10] M. Moretti, A. Todini, and A. Baiocchi. "Distributed radio resource allocation for the downlink of multi-cell OFDMA radio systems." In *Teletraffic Congress (ITC), 2010 22nd International*, pp. 1–7, 2010.

[MTB11] M. Moretti, A. Todini, A. Baiocchi, and G. Dainelli. "A Layered Architecture for Fair Resource Allocation in Multicellular Multicarrier Systems." *Vehicular Technology, IEEE Transactions on*, **60**(4):1788–1798, 2011.

[NDN16] S. Nisana, S. Rao Dasari, and G. B. S. R. Naidu. "Decentralized hierarchical resource allocation algorithm in small cellular networks for an uplink and downlink." In *2016 International Conference on Signal Processing, Communication, Power and Embedded System (SCOPES)*, pp. 236–242, Oct 2016.

[NX15] W. Nasrin and J. Xie. "A self-adaptive handoff decision algorithm for densely deployed closed-group femtocell networks." In *Sensing, Communication, and Networking (SECON), 2015 12th Annual IEEE International Conference on*, pp. 390–398, June 2015.

[P 08] P. Kysti, J. Meinil, L. Hentil, X. Zhao, T. Jms, C. Schneider, M. Narandzi, M. Milojevi, A. Hong, J. Ylitalo, V.M. Holappa, M. Alatossava, R. Bultitude, Y. Jong, T. Rautiainen. "WINNER II Channel Models." *IST-WINNER II Deliverable D1.1.2 Ver 1.2*, Apr 2008.

[PSQ12] E. Pateromichelakis, M. Shariat, A. Ul Quddus, and R. Tafazolli. "Dynamic graph-based multi-cell scheduling for femtocell networks." In *2012 IEEE Wireless Communications and Networking Conference Workshops (WCNCW)*, pp. 98–102, April 2012.

[PSQ13] E. Pateromichelakis, M. Shariat, A. ul Quddus, and R. Tafazolli. "On the Evolution of Multi-Cell Scheduling in 3GPP LTE / LTE-A." *Communications Surveys Tutorials, IEEE*, **15**(2):701–717, 2013.

[QLT17] L. Qiang, J. Li, and C. Touati. "A User Centered Multi-Objective Handoff Scheme for Hybrid 5G Environments." *IEEE Transactions on Emerging Topics in Computing*, **5**(3):380–390, July 2017.

[RSS10a] Abhishek Roy, Jitae Shin, and Navrati Saxena. "Interference Management in OFDMA Femtocells." *Small Cell Forum*, Mar 2010.

[RSS10b] Abhishek Roy, Jitae Shin, and Navrati Saxena. "Interference Management in OFDMA Femtocells." *Small Cell Forum*, Mar 2010.

[SAV12] S. Singh, J.G. Andrews, and G. de Veciana. "Interference Shaping for Improved Quality of Experience for Real-Time Video Streaming." *Selected Areas in Communications, IEEE Journal on*, **30**(7):1259–1269, 2012.

[SH10] S. Sun and R. Huang. "An adaptive k-nearest neighbor algorithm." In *2010 Seventh International Conference on Fuzzy Systems and Knowledge Discovery*, volume 1, pp. 91–94, Aug 2010.

[SYN17] J. Shi, L. Yang, and Q. Ni. "Novel Intercell Interference Mitigation Algorithms for Multicell OFDMA Systems With Limited Base Station Cooperation." *IEEE Transactions on Vehicular Technology*, **66**(1):406–420, Jan 2017.

[THX13] H. Tang, P. Hong, and K. Xue. "HeNB-aided virtual-handover for range expansion in LTE femtocell networks." *Journal of Communications and Networks*, **15**(3):312–320, June 2013.

[VK15] A. Vahabpour and B. H. Khalaj. "Graph-based altruistic games for interference mitigation in femtocell networks." In *2015 IEEE 26th Annual International Symposium on Personal, Indoor, and Mobile Radio Communications (PIMRC)*, pp. 1883–1888, Aug 2015.

[WCT17] F. Wang, W. Chen, H. Tang, and Q. Wu. "Joint Optimization of User Association, Subchannel Allocation, and Power Allocation in Multi-Cell Multi-Association OFDMA Heterogeneous Networks." *IEEE Transactions on Communications*, **65**(6):2672–2684, June 2017.

[WXS06] Lan Wang, Yisheng Xue, and E. Schulz. "Resource Allocation in Multicell OFDM Systems Based on Noncooperative Game." In *Personal, Indoor and Mobile Radio Communications, 2006 IEEE 17th International Symposium on*, pp. 1–5, 2006.

[YD12] E. Yaacoub and Z. Dawy. "A Survey on Uplink Resource Allocation in OFDMA Wireless Networks." *Communications Surveys Tutorials, IEEE*, **14**(2):322–337, 2012.

[YDH12a] Yiwei Yu, E. Dutkiewicz, Xiaojing Huang, and M. Mueck. "Adaptive power allocation for soft frequency reuse in multi-cell LTE networks." In *Communications and Information Technologies (ISCIT), 2012 International Symposium on*, pp. 991–996, 2012.

[YDH12b] Yiwei Yu, E. Dutkiewicz, Xiaojing Huang, and M. Mueck. "A resource allocation scheme for balanced performance improvement in LTE networks with inter-cell interference." In *Wireless Communications and Networking Conference (WCNC), 2012 IEEE*, pp. 1630–1635, 2012.

[YDH13] Yiwei Yu, E. Dutkiewicz, Xiaojing Huang, and M. Mueck. "Downlink Resource Allocation for Next Generation Wireless Networks with Inter-Cell Interference." *Wireless Communications, IEEE Transactions on*, **12**(4):1783–1793, 2013.

[YI03] M. E. Yahia and B. A. Ibrahim. "K-nearest neighbor and C4.5 algorithms as data mining methods: advantages and difficulties." In *ACS/IEEE International Conference on Computer Systems and Applications, 2003. Book of Abstracts.*, pp. 103–, July 2003.

[YY06] X. Yu and X. Yu. "The Research on An Adaptive K-Nearest Neighbors Classifier." In *2006 International Conference on Machine Learning and Cybernetics*, pp. 1241–1246, Aug 2006.

[ZHJ13] L. Zhirong, Q. Hua, Z. Jihong, and X. Xiguang. "User-oriented graph based frequency allocation algorithm for densely deployed femtocell network." *China Communications*, **10**(12):57–65, Dec 2013.

[ZLX16] X. Zhu, M. Li, W. Xia, and H. Zhu. "A novel handoff algorithm for hierarchical cellular networks." *China Communications*, **13**(8):136–147, Aug 2016.

[ZXM14] X. Zhang, Z. Xiao, S. B. Mahato, E. Liu, B. Allen, and C. Maple. "Dynamic user equipment-based hysteresis-adjusting algorithm in LTE femtocell networks." *IET Communications*, **8**(17):3050–3060, 2014.